Journal of Organometallic Chemistry 901 (2019) 120938

Contents lists available at ScienceDirect

Journal of Organometallic Chemistry

journal homepage: www.elsevier.com/locate/jorganchem

C–C coupling of CH activated polar vinyl monomers by a pentaruthenium cluster complex☆

Richard D. Adams*, Claire M. Prince, Mark D. Smith, Jonathan D. Tedder, Nutan D. Wakdikar

Department of Chemistry and Biochemistry, University of South Carolina, Columbia, SC, 29208, USA

ARTICLE INFO

Article history:
Received 13 August 2019
Received in revised form
10 September 2019
Accepted 15 September 2019
Available online 16 September 2019

Keywords:
Ruthenium clusters
C
C bond formation
Olefin coupling
Olefin dimerization
Polar vinyl monomers
Methyl acrylate
N,N-dimethylacrylamide
Vinyl acetate

ABSTRACT

Reactions of $Ru_5(CO)_{15}(\mu_5\text{-}C)$, **1** with the polar vinyl monomers (PVM), methyl acrylate, vinyl acetate and N,N-dimethylacrylamide proceed by cluster opening additions accompanied by CH activation in the vinyl group of the PVM to yield olefin-activated complexes such as $Ru_5(\mu_5\text{-}C)(CO)_{14}[\eta^2\text{-}O{=}CO(Me)CH{=}CH](\mu\text{-}H)$, **2**, $Ru_5(\mu_5\text{-}C)(CO)_{14}[\eta^2\text{-}(MeCO_2)C{=}CH_2](\mu\text{-}H)$, **3** and $Ru_5(\mu_5\text{-}C)(CO)_{14}[\eta^2\text{-}O{=}C(NMe_2)CH{=}CH](\mu\text{-}H)$, **6**. In this work we have investigated the nature of the addition and coupling/cross-coupling of a second PVM to the CH activated PVM in the complexes **2**, **3**, and **6**. The products consist of C–C coupled diolefin complexes that have been transformed into η^3-allyl ligands by shifts of the hydrogen atoms in the C–C coupled ligands. Nine new complexes of $Ru_5(\mu_5\text{-}C)(CO)_{13}[\eta^3\text{-}1\text{-}anti,\ 3\text{-}anti\text{-}(MeO)C{=}O{-}C_3H_3\text{-}\eta^1\text{-}O{=}C(OMe)CH_2](\mu\text{-}H)$, **8**; $Ru_5(\mu_5\text{-}C)(CO)_{13}[\eta^3\text{-}1\text{-}anti,\ 3\text{-}syn\text{-}(MeO_2C)CH_2C_3H_3{-}CH_2\text{-}\eta^1\text{-}O{=}C(OMe)](\mu\text{-}H)$, **9**; $Ru_5(\mu_5\text{-}C)(CO)_{12}[\mu\text{-}\eta^3\text{-}O{=}C(OMe)CH{=}CH][\eta^2\text{-}CH{=}CHCO_2Me](\mu\text{-}H)$, **10**; $Ru_5(\mu_5\text{-}C)(CO)_{13}[\eta^3\text{-}1\text{-}syn,\ 3\text{-}anti\text{-}(MeO_2C)C_3H_3\text{-}\eta^1\text{-}O{=}C(OMe)CH_2](\mu\text{-}H)$, **11**; $Ru_5(\mu_5\text{-}C)(CO)_{13}[\eta^3\text{-}1\text{-}syn,\ 3\text{-}anti\text{-}Me_2NC{=}O{-}C_3H_3\text{-}\eta^1\text{-}O{=}CNMe_2CH_2](\mu\text{-}H)$, **12**; $Ru_5(\mu_5\text{-}C)(CO)_{13}[\eta^3\text{-}1\text{-}anti,\ 3\text{-}syn\text{-}(Me_2N)C(=O){-}C_3H_3{-}CH_2\text{-}\eta^1\text{-}O{=}C(NMe_2)](\mu\text{-}H)$, **13**; $Ru_5(\mu_5\text{-}C)(CO)_{12}[\mu\text{-}\eta^3\text{-}O{=}C(NMe_2)CH{=}CH][\eta^2\text{-}CH{=}CHCO_2Me](\mu\text{-}H)$, **14**; $Ru_5(\mu_5\text{-}C)(CO)_{13}[\eta^3\text{-}1\text{-}anti,\ 3\text{-}syn\text{-}MeO_2CCH_2C_3H_3\text{-}\eta^1\text{-}O{=}C(NMe_2)](\mu\text{-}H)$, **15**, and $Ru_5(\mu_5\text{-}C)(CO)_{12}[\mu\text{-}\eta^2\text{-}(MeO_2C)CH{=}CH][\eta^3\text{-}CH_2{=}CHOC(=O)Me)](\mu\text{-}H)$, **16** have been obtained and structurally characterized. Three of these complexes (**10**, **14** and **16**) contain uncoupled olefin ligands.

1. Introduction

The coupling of carbon – carbon bonds between polar vinyl monomers, such as acrylates, acrylamides, acrylonitrile and vinyl acetate, is used to provide a variety of valuable polymers [1,2]. There has been much interest in developing methods for the polymerization and copolymerization of polar vinyl monomers by using organometallic catalysts [2–4]. The synthesis of dimers of acrylates and acrylamides has also attracted interest because of their potential for use as precursors to adipic acid which is used in the synthesis of nylon-6,6 [5].

Recent studies have shown that metal-based olefinic CH activations can play an important role in the oligomerizations and cross-couplings of certain polar olefins [6,7]. For example, the cross coupling of vinyl carboxylates with acrylates by using palladium acetate catalysts is believed to begin by CH activation on the vinyl group, followed by C–C coupling through insertion and reductive elimination, Scheme 1 [7]. CH activation on the vinyl group of acrylates is often accompanied by coordination of the ester group [8].

In recent studies, we have shown that the square-pyramidal polynuclear metal carbonyl cluster complex $Ru_5(CO)_{15}(\mu_5\text{-}C)$, **1** is able to activate one of the olefinic CH bonds of the vinyl group of methyl acrylate and vinyl acetate to yield the complexes $Ru_5(\mu_5\text{-}C)(CO)_{14}[\eta^2\text{-}O{=}CO(Me)CH{=}CH](\mu\text{-}H)$, **2** and $Ru_5(\mu_5\text{-}C)(CO)_{14}[\eta^2\text{-}(MeCO_2)C{=}CH_2](\mu\text{-}H)$, **3** respectively [9]. Both of these reactions involve opening of the Ru_5 cluster by cleavage of one of the Ru–Ru bonds and is accompanied by loss of a CO ligand that facilitates the addition of the olefin to the complex and its subsequent oxidative addition of the selected CH bond to a metal atom. The choice of the CH bond for activation seems to be determined by the nature substituent on the olefin via the formation of a five-membered chelate ring involving that substituent in the product complex, **2** or **3**, see Scheme 2, [9]. More importantly, we have found that the complexes **2** and **3** will add ethylene and couple it to the activated

☆ Dedicated to Professor Jean-François Halet on the occasion of his 60th birthday.

* Corresponding author.
E-mail address: ADAMSRD@mailbox.sc.edu (R.D. Adams).

https://doi.org/10.1016/j.jorganchem.2019.120938
0022-328X/

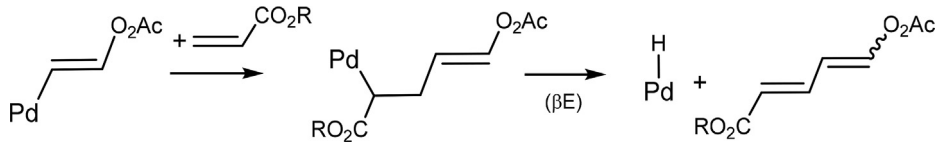

Scheme 1. A mechanism proposed for the Pd-catalyzed cross-coupling of vinyl acetate with alkyl acrylates [7].

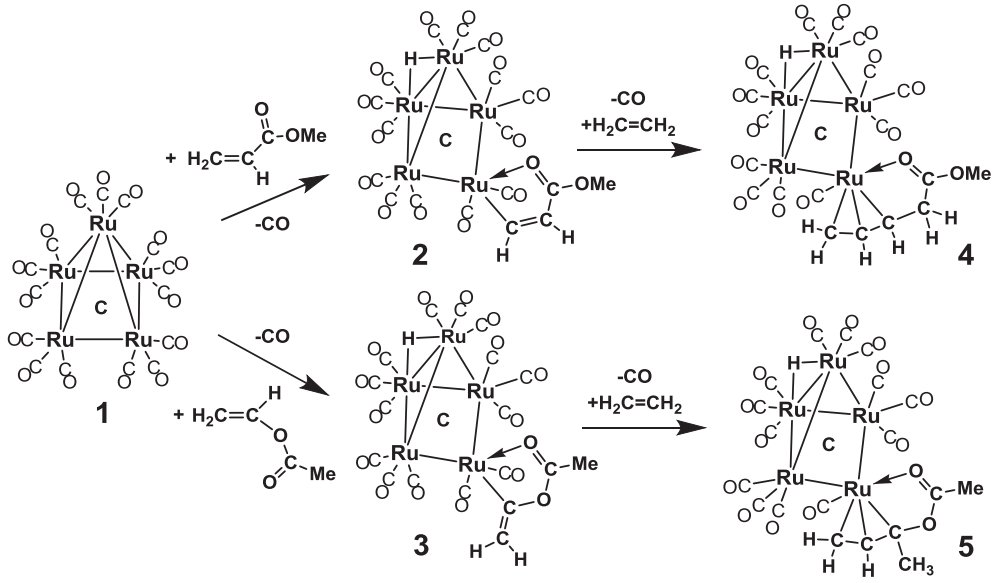

Scheme 2. A schematic of the cluster opening and CH activation in the vinyl groups of methyl acrylate and vinyl acetate and the addition and coupling of ethylene to those products.

olefinic ligand at the CH bond activation site to yield the products $Ru_5(\mu_5\text{-}C)(CO)_{13}[\eta^4\text{-}anti\text{-}O{=}C(OMe)CH_2CHCHCH_2](\mu\text{-}H)$, **4** and $Ru_5(\mu_5\text{-}C)(CO)_{13}[\eta^4\text{-}1,1\text{-}anti\text{-}syn\text{-}[(MeCO_2)C(Me)CHCH_2](\mu\text{-}H)$, **5** among others that contain substituted η^3-allyl ligands, Scheme 2 [10].

In a continuation of this work, we have now investigated the reactions of **1**, **2**, **3** and $Ru_5(\mu_5\text{-}C)(CO)_{14}[\eta^2\text{-}O{=}C(NMe_2)CH{=}CH](\mu\text{-}H)$, **6** [12] with additional quantities of methyl acrylate, N,N-dimethylacrylamide, and vinyl acetate. Products containing C—C coupled versions of the olefins which are coordinated to the Ru_5 cluster through η^3-allylic binding arrangements were obtained. The results of these studies are reported here.

2. Experimental section

2.1. General data

All reactions were performed under an atmosphere of nitrogen. Reagent grade solvents were dried by standard procedures and were freshly distilled prior to use. Infrared spectra were recorded on a Thermo Scientific Nicolet IS10. ^{1}H NMR spectra were recorded on a Varian Mercury 300 spectrometer operating at 300.1 MHz or on a Bruker AVANCE III spectrometer operating at 400 MHz. Mass spectrometric (MS) measurements were performed by a direct-exposure probe by using electron impact (EI) ionization. $Ru_3(CO)_{12}$ was purchased from STREM and was used without further purification. $Ru_5(\mu_5\text{-}C)(CO)_{15}$, **1** was prepared from $Ru_3(CO)_{12}$ according to a previously reported procedure [11]. Methyl acrylate, N,N-dimethylacrylamide (DMA), vinyl acetate and trimethylamine-N-oxide, (Me_3NO) were purchased from Sigma-Aldrich and were used without further purification. Product separations were performed by TLC in air on Analtech 0.25 mm and 0.50 mm silica gel 60 Å F254 glass plates.

2.2. Reaction of 1 with DMA at 98 °C

25.2 mg (0.027 mmol) of **1** was added to a 50 mL three-neck flask in 20 mL of degassed heptane with 8 μL of DMA. After heating for 6.5 h at 98 °C, the solvent was removed *in vacuo*, and the products were then isolated by TLC by using a hexane/methylene chloride mixture to provide in the order of elution: 8.0 mg (29% yield) of $Ru_5(\mu_5\text{-}C)(CO)_{14}[\eta^2\text{-}O{=}C(NMe_2)CH{=}CH](\mu\text{-}H)$, **6** [12] and 1.2 mg (5% yield) of $Ru_5(\mu_5\text{-}C)(CO)_{13}[\mu\text{-}\eta^3\text{-}O{=}C(NMe_2)CHCH](\mu\text{-}H)$, **7a** [12]. Compound **7a** was obtained previously from the reaction of $Ru_5(\mu_5\text{-}C)(CO)_{13}(NHMe_2)[\eta^2\text{-}O{=}C(NMe_2)](\mu\text{-}H)$, with C_2H_2 and compound **6** was obtained previously by the carbonylation (using CO) of **7a** at room temperature [12].

2.3. Reaction of $Ru_5(\mu_5\text{-}C)(CO)_{14}[\eta^2\text{-}O{=}C(OMe)CH{=}CH](\mu\text{-}H)$ 2 with methyl acrylate in the presence of trimethylamine N-oxide at 25 °C

39.8 mg (0.040 mmol) of **2** was added to a 50 mL three-neck flask in 20 mL of degassed hexane with 300 μL of methyl acrylate and 16 mg (0.21 mmol) of trimethylamine N-oxide. After stirring for 20 h at room temperature, the solvent was removed *in vacuo*, and the products were then isolated by TLC by using a hexane/methylene chloride mixture to provide in the order of elution: 2.7 mg (7% yield) of unreacted starting material, **2**, 3.3 mg (8%) of $Ru_5(\mu_5\text{-}C)(CO)_{13}[\mu\text{-}\eta^3\text{-}O{=}C(OMe)CHCH](\mu\text{-}H)$, **7b**, [10]; 3.6 mg (8% yield) of $Ru_5(\mu_5\text{-}C)(CO)_{13}[\eta^3\text{-}1\text{-}anti,\ 3\text{-}anti\text{-}(MeO)C{=}O{-}C_3H_3\text{-}\eta^1\text{-}O{=}C(OMe)CH_2](\mu\text{-}H)$, **8**, 5.6 mg (13% yield) of $Ru_5(\mu_5\text{-}C)(CO)_{13}[\eta^3\text{-}1\text{-}anti,\ 3\text{-}syn\text{-}(MeO_2C)CH_2C_3H_3{-}CH_2\text{-}\eta^1\text{-}O{=}C(OMe)](\mu\text{-}H)$, **9**, 2.8 mg (7% yield) of $Ru_5(\mu_5\text{-}C)(CO)_{12}[\mu\text{-}\eta^3\text{-}O{=}C(OMe)CH{=}CH][\eta^2\text{-}$

CH=CHCO$_2$Me](μ-H), **10**, and 3.7 mg (9% yield) of Ru$_5$(μ$_5$-C)(CO)$_{13}$[η^3-1-*syn*, 3-*anti*-(MeO$_2$C)C$_3$H$_3$-η^1-O=C(OMe)CH$_2$](μ-H), **11**. Spectral data for **8**: IR νCO (cm^{-1} in hexane) 2090(w), 2060(s), 2051(vs), 2036(w), 2019(m), 2006(w), 1993(vw), 1985(vw), 1970(vw). ^{1}H NMR (CD$_2$Cl$_2$, in ppm) δ = 5.71 (t, $^3J_{H-H}$ = 8 Hz, 1H, C−CH$_2$−C(**H**)−C(H)−C(H)), 5.22 (d, $^3J_{H-H}$ = 8 Hz, 1H, C−CH$_2$−C(H)−C(H)−C(**H**), 4.32 (t, $^3J_{H-H}$ = 8 Hz, 1H, C−CH$_2$−C(H)−C(**H**)−CH), 3.59 (s, 3H, OMe), 3.41 (dd, $^3J_{H-H}$ = 8 Hz, $^2J_{H-H}$ = 20 Hz, 1H, C−C**H$_2$**−C(H)−C(H)−CH), 3.37 (s, 3H, OMe), 3.15 (d, $^2J_{H-H}$ = 20 Hz, 1H, C−C**H$_2$**−C(H)−C(H)−CH), −22.12 (s, 1H, hydride). EI/MS *m*/*z*. 1053.6. The isotope distribution is consistent with the presence of five ruthenium atoms. Spectral data for **9**: IR νCO (cm^{-1} in hexane) 2090(w), 2060(m), 2051(vs), 2036(w), 2020(m), 2003(w), 1994(vw), 1986(vw), 1970(vw). ^{1}H NMR (CD$_2$Cl$_2$, in ppm) δ = 5.48 (d, $^3J_{H-H}$ = 7 Hz, 1H, C−C(**H**)−C(H)−C(H)−CH$_2$, 5.09 (dd, $^3J_{H-H}$ = 7 Hz, $^3J_{H-H}$ = 11 Hz, 1H, C−C(H)−C(**H**)−CH−CH$_2$, 3.96 (dd, $^3J_{H-H}$ = 4 Hz, $^2J_{H-H}$ = 16 Hz, 1H, C−C(H)−C(H)−C(H)−C**H$_2$**, 3.78 (s, 3H, OMe), 3.41, (s, 3H, OMe), 3.39 (td, $^3J_{H-H}$ = 4 Hz, $^3J_{H-H}$ = 11 Hz, 1H, C−C(H)−C(H)−C(**H**)−CH$_2$, 3.14 (dd, $^3J_{H-H}$ = 10 Hz, $^2J_{H-H}$ = 16 Hz, 1H, C−C(H)−C(H)−C(H)−C**H$_2$**, -22.43 (s, 1H, hydride). ESI/MS m^+/*z*. 1054.3. Spectral data for **10**: IR νCO (cm^{-1} in hexane) 2093(m), 2066(vs), 2050(s), 2032(m), 2026(m), 2017(w), 2004(vw), 1997(w), 1992(sh). ^{1}H NMR (CD$_2$Cl$_2$, in ppm) δ = 11.17 (d, $^3J_{H-H}$ = 5 Hz, 1H, Ru−C(**H**)=CH), 4.46 (d, $^3J_{H-H}$ = 5 Hz, 1H, Ru−C(H)=C**H**), 4.03 (dd, $^3J_{H-H}$ = 8 Hz, $^3J_{H-H}$ = 11 Hz, 1H, C(H$_2$) = C**H**), 3.83 (s, 3H, OMe), 3.81 (d, $^3J_{H-H}$ = 11 Hz, 1H, C**H$_2$**=C(H)), 3.41 (s, 3H, OMe), 2.34 (d, $^3J_{H-H}$ = 8 Hz, 1H, C**H$_2$**=CH), −20.92 (s, 1H, hydride). EI/MS *m*/*z*. 1025.4. The isotope distribution is consistent with the presence of five ruthenium atoms. Spectral data for **11**: IR νCO (cm^{-1} in hexane) 2090(w), 2060(s), 2051(vs), 2037(w), 2020(m), 2002(w), 1994(vw), 1986(vw), 1974(vw), 1970(vw), 1966(vw). ^{1}H NMR (CD$_2$Cl$_2$, in ppm) δ = 5.45 (t, $^3J_{H-H}$ = 8 Hz, 1H, C−C(H$_2$)−C(**H**)−C(H)−C(H), 5.35 (dd, $^3J_{H-H}$ = 4 Hz, $^3J_{H-H}$ = 12 Hz, 1H, C−C(H**$_2$**)−C(H)−C(**H**)−C(H), 3.86 (s, 3H, OMe), 3.49 (s, 3H, OMe), 3.42 (dd, $^3J_{H-H}$ = 8 Hz, $^2J_{H-H}$ = 20 Hz, 1H, C−C(**H$_2$**)−C(H)−C(H)−C(H), 2.80 (d, $^3J_{H-H}$ = 12 Hz, 1H, C−C(H**$_2$**)−C(H)−C(H)−C(**H**), 2.69 (d, $^2J_{H-H}$ = 20 Hz, 1H, C−C(**H$_2$**)−C(H)−C(H)−C(H), −22.16 (s, 1H, hydride). EI/MS *m*/*z*. 1054.4. The isotope distribution is consistent with the presence of five ruthenium atoms.

2.4. Reaction of Ru$_5$(μ$_5$-C)(CO)$_{14}$[η^2-O=C(NMe)$_2$CH=CH](μ-H), 6 with DMA at 80 °C

22.3 mg (0.022 mmol) of **6** was added to a 50 mL three-neck flask in 20 mL of degassed benzene with 200 μL of DMA. After heating for 11.5 h at 98 °C, the solvent was removed *in vacuo*, and the products were then isolated by TLC by using a hexane/methylene chloride mixture to provide in the order of elution: 3.2 mg (14%) of unreacted starting material **6**; 4.7 mg (22% yield) of Ru$_5$(μ$_5$-C)(CO)$_{13}$[μ-η^3-O=C(NMe$_2$)CHCH](μ-H), **7a**; 4.3 mg (18% yield) of Ru$_5$(μ$_5$-C)(CO)$_{13}$[η^3-1-*syn*, 3-*anti*-Me$_2$NC=O−C$_3$H$_3$-η^1-O=CNMe$_2$CH$_2$](μ-H), **12** and 5.2 mg (22% yield) of Ru$_5$(μ$_5$-C)(CO)$_{13}$[η^3-1-*anti*, 3-*syn*-(Me$_2$N)C(=O)−C$_3$H$_3$−CH$_2$-η^1-O=C(NMe$_2$)](μ-H), **13**. Spectral data for **12**: IR νCO (cm^{-1} in dichloromethane) 2087(m), 2059(s), 2044(vs), 2032(sh), 2014(m), 1973(w). ^{1}H NMR (CD$_2$Cl$_2$, in ppm) δ = 5.48 (d, $^3J_{H-H}$ = 7 Hz, 1H, C−C(**H**)−C(H)−C(H)−CH$_2$), 4.96 (dd, $^3J_{H-H}$=7 Hz; $^3J_{H-H}$, = 11 Hz, 1H, C−C(H)−C(**H**)−C(H)−CH$_2$, 4.04 (dd, $^3J_{H-H}$ = 4 Hz; $^2J_{H-H}$ = 16 Hz, 1H, C−C(H)−C(H)−C(H)−C**H$_2$**, 3.31 (td, $^3J_{H-H}$ = 4 Hz; $^3J_{H-H}$ = 10 Hz, 1H, C−C(H)−C(H)−C(**H**)−CH$_2$, 3.14 (s, 3H, NMe$_2$), 3.11 (s, 3H, NMe$_2$), 3.01 (dd, $^3J_{H-H}$ = 10 Hz; $^2J_{H-H}$ = 16 Hz, 1H, C−C(H)−C(H)−C(H)−C(**H$_2$**), 2.99 (s, 3H, NMe$_2$, 2.44 (s, 3H, NMe$_2$), −22.43 (s, 1H, hydride). EI/MS *m*/*z*. 1082. The isotope distribution is consistent with the presence of five ruthenium atoms. Spectral data for **13**: IR νCO (cm^{-1} in dichloromethane) 2086(m), 2056(s), 2044(vs), 2032(sh), 2014(m), 1973(w). ^{1}H NMR (CD$_2$Cl$_2$, in ppm) δ = 5.54 (mm, 2H, C−C(s, 3H, NMe)$_2$), 3.17 (d, $^3J_{H-H}$ = 10 Hz, 1H, C−C(**H**)−C(H)−C(H)−CH$_2$), 3.06 (s, 3H, NMe$_2$), 2.80 (s, 3H, NMe$_2$), 2.71 (d, $^2J_{H-H}$ = 19 Hz, 1H, C−C(H)−C(H)−C(H)−C**H$_2$**), 2.57 (s, 3H, NMe$_2$), −22.23 (s, 1H, hydride). EI/MS *m*/*z*. 1081. The isotope distribution is consistent with the presence of five ruthenium atoms.

2.5. Synthesis of Ru$_5$(μ$_5$-C)(CO)$_{12}$[μ-η^3-O=C(NMe$_2$)CH=CH][η^2-CH=CHCO$_2$Me](μ-H), 14 and Ru$_5$(μ$_5$-C)(CO)$_{13}$[η^3-1-anti, 3-syn-MeO$_2$CCH$_2$C$_3$H$_3$-η^1-O=C(NMe$_2$)](μ-H), 15 from the reaction of 6 with methyl acrylate at 80 °C

20.4 mg (0.020 mmol) of **6** was added to a 50 mL three-neck flask in 25 mL of degassed benzene with 600 μL of methyl acrylate. After heating for 46 h at 80 °C, the solvent was removed *in vacuo*, and the products were then isolated by TLC by using a hexane/methylene chloride mixture to provide in the order of elution: 0.7 mg (3% yield) of **2**, 4.0 mg (20% yield) of starting material **6**, 0.4 mg (2% yield) of **7a**, 0.7 mg (3% yield) of Ru$_5$(μ$_5$-C)(CO)$_{12}$[μ-η^3-O=C(NMe$_2$)CH=CH][η^2-CH=CHCO$_2$Me](μ-H), **14**, and 6.5 mg (30% yield) of Ru$_5$(μ$_5$-C)(CO)$_{13}$[η^3-1-*anti*, 3-*syn*-MeO$_2$CCH$_2$C$_3$H$_3$-η^1-O=C(NMe$_2$)](μ-H), **15**. Spectral data for **14**: IR νCO (cm^{-1} in hexane) 2090(m), 2063(vs), 2046(s), 2028(m), 2024(sh), 2014(w). ^{1}H NMR (CD$_2$Cl$_2$, in ppm) δ = 11.14 (d, $^3J_{H-H}$ = 5 Hz, 1H, Ru−C(**H**)=C(H)−C), 4.61 (d, $^3J_{H-H}$ = 5 Hz, 1H, Ru−C(H)=C(**H**)−C), 4.01 (dd, $^3J_{H-H}$ = 8 Hz, $^3J_{H-H}$ = 11 Hz, 1H, C(H$_2$)−C(**H**)), 3.8 (s, 3H, OMe), 3.73 (d, $^3J_{H-H}$ = 11 Hz, 1H, C(**H$_2$**)−C(H)), 3.0 (s, 3H, NMe$_2$), 2.4 (s, 3H, NMe$_2$), 2.31 (d, $^3J_{H-H}$ = 8 Hz, 1H, C(**H$_2$**)−C(H)), −20.947 (s, 1H, hydride). EI/MS *m*/*z*. 1009 (M$^+$), 953 (M$^+$ − 2CO). Spectral data for **15**: IR νCO (cm^{-1} in hexane) 2089(w), 2061(s), 2048(vs), 2035(w), 2019(m), 2006(vw), 1990(vw), 1979(w), 1967(vw), 1948(vw). ^{1}H NMR (CD$_2$Cl$_2$, in ppm) δ = 5.49 (d, $^3J_{H-H}$ = 7 Hz, 1H, C−C(**H**)−C(H)−C(H)−C(H$_2$), 4.97 (dd, $^3J_{H-H}$ = 7 Hz, $^3J_{H-H}$ = 11 Hz, 1H, C−C(H)−C(**H**)−C(H)−C(H$_2$), 3.92 (dd, $^3J_{H-H}$ = 4 Hz, $^2J_{H-H}$ = 16 Hz, 1H, C−C(H)−C(H)−C(H)−C(**H$_2$**), 3.78 (s, 3H, OMe), 3.13 (s, 3H, NMe), 2.45 (s, 3H, NMe), −22.23 (s, 1H, hydride). EI/MS *m*/*z*. 1066.7. The isotope distribution is consistent with the presence of five ruthenium atoms.

2.6. Synthesis of Ru$_5$(μ$_5$-C)(CO)$_{12}$[μ-η^2-(MeO$_2$C)CH=CH][η^3-CH$_2$=CHOC(=O)Me)](μ-H), 16 from the reaction of 3 with vinyl acetate

23.0 mg (0.023 mmol) of **3** was added to a 50 mL three-neck flask in 25 mL of degassed hexane with 250 μL of vinyl acetate and 11.0 mg (0.15 mmol) of trimethylamine N-oxide. After stirring at room temperature for 15.5 h, the solvent was removed *in vacuo*, and the products were then isolated by TLC by using a hexane/methylene chloride solvent mixture to provide in the order of elution: 0.6 mg (3% yield) of Ru$_5$(μ$_5$-C)(CO)$_{12}$[μ-η^2-(MeO$_2$C)CH=CH][η^3-CH$_2$=CHOC(=O)Me)](μ-H), **16**. Spectral data for **16**: IR νCO (cm^{-1} in hexane) 2088(w), 2063(s), 2045(vs), 2026(w), 2012(m), 2009(vw), 1992(vw), 1982(vw). ^{1}H NMR (CD$_2$Cl$_2$, in ppm) δ = 10.51 (d, ^3J = 9 Hz, 1H, O−C(H)=C(**H**)−Ru), 6.92 (dd, ^3J = 5 Hz, ^3J = 7 Hz, 1H, O−C(H)=C(**H$_2$**), 6.06 (d, ^3J = 9 Hz, 1H, O−C(**H**)=C(H)−Ru), 3.66 (t, ^3J = 5 Hz, 1H, O−C(H)=C(**H$_2$**), 3.34 (dd, ^3J = 5 Hz, ^3J = 7 Hz, 1H, O−C(H)=C(**H$_2$**), 2.13 (s, 3H, C=O(Me), 1.72 (s, 3H, C=O(Me), −21.40 (s, 1H, hydride). EI/MS *m*/*z*. 1025.3. The isotope distribution is consistent with the presence of five ruthenium atoms.

2.7. Isomerization of compound 8 at 80 °C

3.6 mg (0.004 mmol) of **8** was added to a NMR tube in 1.5 mL of d$_8$-toluene. The progress of the reaction was monitored by ^{1}H NMR spectroscopy. After heating for 25 h at 80 °C in a temperature-

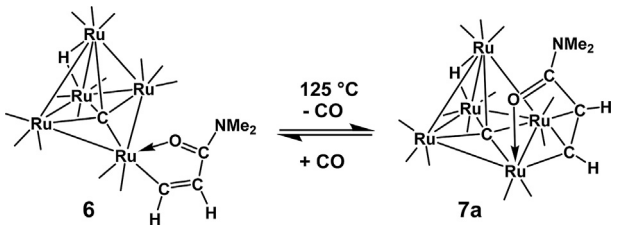

Scheme 3. A schematic of the structures of compounds **6** and **7a** showing their interconversions.

controlled oil bath, the solution was allowed to cool to room temperature and the solvent was removed under a stream of nitrogen. The product was then isolated by TLC by using a hexane/methylene chloride solvent mixture to provide 2.6 mg (72% yield) of **11**.

2.8. Isomerization of compound 9 at 80 °C

4.7 mg (0.003 mmol) of **9** was added to a NMR tube in 1.5 mL of d_8-toluene. After heating for 34 h at 80 °C in a temperature-controlled silicone oil bath. The progress of the reaction was monitored by ^{1}H NMR spectroscopy. The solution was allowed to cool and the solvent was removed under a stream of nitrogen. The product was then isolated by TLC with a hexane/methylene chloride mixture to provide 3.0 mg (64% yield) of **11**.

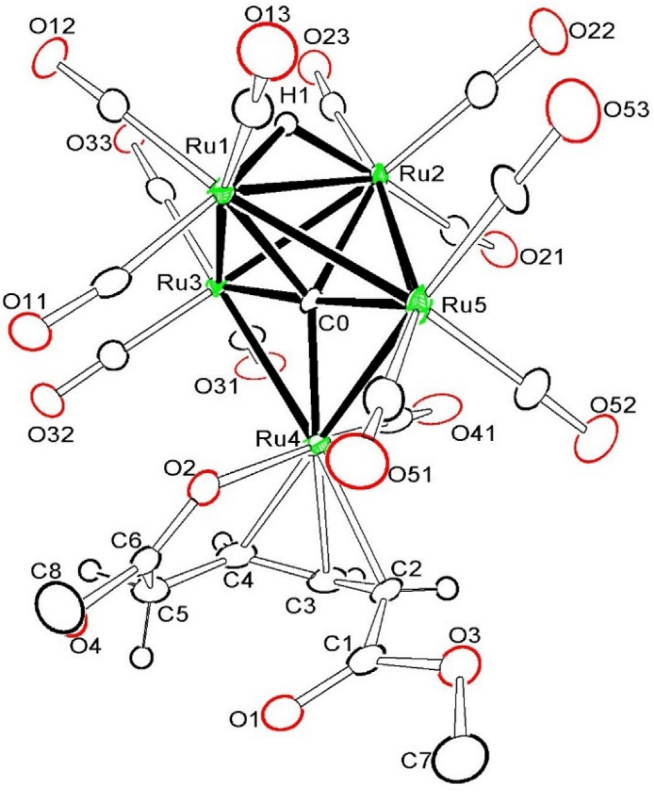

Fig. 1. ORTEP diagram of the molecular structure of $Ru_5(\mu_5\text{-}C)(CO)_{13}[\eta^3\text{-}1\text{-}anti, 3\text{-}anti\text{-}(MeO)C{=}O{-}C_3H_3\text{-}\eta^1\text{-}O{=}C(OMe)CH_2](\mu\text{-}H)$, **8** showing 40% thermal ellipsoid probability. The hydrogen atoms on the methyl groups are omitted for clarity. Selected interatomic bond distances (Å) are as follows: Ru1−Ru3 = 2.8233(6), Ru1−Ru5 = 2.8483(6), Ru1−Ru2 = 2.8498(6), Ru2−Ru5 = 2.8626(6) Ru2−Ru3 = 2.8793(6), Ru3−Ru4 = 2.9183(6), Ru4−Ru5 = 2.9005(7), Ru1−H1 = 1.59(7), Ru2−H1 = 1.72(7), Ru4−O2 = 2.170(4), Ru4−C2 = 2.225(6), Ru4−C3 = 2.175(6), Ru4−C4 = 2.258(6), C1−C2 = 1.484(9), C2−C3 = 1.419(9), C3−C4 = 1.396(9), C4−C5 = 1.501(9), C6−O2 = 1.247(7), Ru1−C0 = 2.131(5).

2.9. Crystallographic analyses

Single crystals of compounds **8**–**16** suitable for X-ray diffraction analyses were obtained by slow evaporation of solvent from solutions of the pure compounds. X-ray intensity data for compounds **11** and **13** was measured by using a Bruker SMART APEX CCD-based diffractometer by using Mo K_α radiation ($\lambda = 0.71073$ Å). The raw data frames were integrated by using the program SAINT + by using a narrow-frame integration algorithm [13]. Correction for Lorentz and polarization effects were also applied with SAINT+ [13]. An empirical absorption correction based on the multiple measurements of equivalent reflections was applied by using the program SADABS in each analysis [13]. X-ray intensity data for compounds **8**–**10**, **12** and **14**–**16** were measured by using a Bruker D8 QUEST diffractometer equipped with a PHOTON-100 CMOS area detector and an Incoatec microfocus source (Mo Kα radiation, $\lambda = 0.71073$ Å) [14]. All structures were solved by a combination of direct methods and difference Fourier syntheses, and refined by full-matrix least squares on F^2 by using the SHELXTL software package [15]. Crystal data, data collection parameters, and results for each analysis are summarized in Table S1 – S3, see Electronic Supporting Information.

3. Results and discussion

The reaction of **1** with N,N-dimethylacrylamide (DMA), $CH_2{=}C(H)C(=O)NMe_2$, in heptane solvent at reflux (98 °C) for 6.5 h yielded two products: $Ru_5(\mu_5\text{-}C)(CO)_{14}[\eta^2\text{-}O{=}C(NMe_2)CH{=}CH](\mu\text{-}H)$, **6** in 29% yield and $Ru_5(\mu_5\text{-}C)(CO)_{13}[\mu\text{-}\eta^3\text{-}O{=}C(NMe_2)CHCH](\mu\text{-}H)$, **7a** in 5% yield. Compounds **6** and **7a** were obtained previously albeit in lower yields from reactions of the formamido complex $Ru_5(\mu_5\text{-}C)(CO)_{14}[\eta^2\text{-}O{=}C(NMe_2)](\mu\text{-}H)$ with C_2H_2 [12]. They are easily interconverted by the elimination and addition of CO, Scheme 3.

The reaction of **2** with an excess methyl acrylate in the presence of Me_3NO at room temperature for 20 h yielded five Ru_5C complexes: $Ru_5(\mu_5\text{-}C)(CO)_{13}[\mu\text{-}\eta^3\text{-}O{=}CO(Me)CHCH](\mu\text{-}H)$, **7b** in 8% yield, $Ru_5(\mu_5\text{-}C)(CO)_{13}[\eta^3\text{-}1\text{-}anti, 3\text{-}anti\text{-}(MeO)C{=}O{-}C_3H_3\text{-}\eta^1\text{-}O{=}C(OMe)CH_2](\mu\text{-}H)$, **8** in 8% yield, $Ru_5(\mu_5\text{-}C)(CO)_{13}[\eta^3\text{-}1\text{-}anti, 3\text{-}syn\text{-}(MeO_2C)CH_2C_3H_3{-}CH_2\text{-}\eta^1\text{-}O{=}C(OMe)](\mu\text{-}H)$, **9** in 13% yield, $Ru_5(\mu_5\text{-}C)(CO)_{12}[\mu\text{-}\eta^3\text{-}O{=}C(OMe)CH{=}CH][\eta^2\text{-}CH{=}CHCO_2Me](\mu\text{-}H)$, **10** in 7% yield, and $Ru_5(\mu_5\text{-}C)(CO)_{13}[\eta^3\text{-}1\text{-}syn, 3\text{-}anti\text{-}(MeO_2C)C_3H_3\text{-}\eta^1\text{-}O{=}C(OMe)CH_2](\mu\text{-}H)$, **11** in 9% yield. Three of these complexes **8**, **9** and **11** were formed by a tail-to-tail coupling of two methyl acrylate units. Compound **7b** was obtained in previous studies [10]. It is a simple decarbonylation product of **2** that is structurally similar to **7a** except that it contains an OMe group in the place of the NMe_2 group in **7a**.

Compounds **8**–**11** were characterized by a combination of IR, ^{1}H NMR, mass spectrometry and single-crystal X-ray diffraction analyses. Compounds **8**, **9**, and **11** are isomers formed by the addition of one equivalent of methyl acrylate to **2** combined with a tail-to-tail coupling of two acrylate ligands at the bridging Ru atom, Ru4, of the metal cluster. An ORTEP diagram of the molecular structure of **8** is shown in Fig. 1. Compound **8** consists of an open square pyramidal cluster of five metal atoms with thirteen linear terminal carbonyl ligands and a bridging hydrido ligand across the Ru1 − Ru2 bond, Ru1−H1 = 1.59(7) Å, Ru2−H1 = 1.72(7) Å, $\delta = -22.12$. The most interesting ligand in **8** is a disubstituted η^3-allyl ligand, $(MeO_2C)CH_2C_3H_3CH_2\text{-}\eta^1\text{-}O{=}C(OMe)$. Atoms C2, C3, and C4 represent the coordinated allyl portion of this ligand which was formed by a tail-to-tail coupling of two methyl acrylate molecules at the carbon atoms C3 and C4, C3−C4 = 1.396(9) Å and C2−C3 = 1.419(9) Å, on

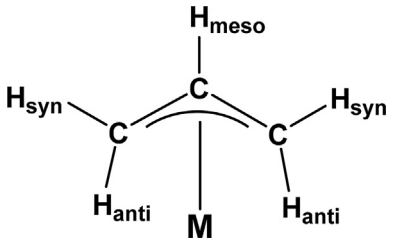

Scheme 4. Stereochemical definitions of η^3-coordinated allyl ligands [16].

the bridging metal atom Ru4, Ru4–C2 = 2.225(6) Å, Ru4–C3 = 2.175(6) Å, Ru4–C4 = 2.258(6) Å. The two substituents exhibit an 1-*anti*,3-*anti* stereochemistry, i.e. the three H atoms of the η^3-allyl group are cis to each other, $^3J_{H\text{-}H} = 8$ Hz; the substituents are anti to the meso hydrogen at the carbon 2-position, see Scheme 4 for the stereochemical definitions of η^3-coordinated allyl ligands [16].

There is a five-membered ring composed of the atoms Ru4–O2–C6–C5–C4 that contains a methylene group at the C5 location, $^2J_{H\text{-}H} = 20$ Hz, for the inequivalent H atoms that are attached to it. This group was presumably formed by a metal-mediated hydrogen shift from the β-carbon to the α-carbon of one of the methyl acrylate units in course of the C–C bond forming process.

An ORTEP diagram of the molecular structure of **9** is shown in Fig. 2. Compound **9** is an isomer of **8** in which the two methyl acrylate units are coupled to form a disubstituted η^3- $(MeO_2C)CH_2C_3H_3CH_2$-η^1-O=C(OMe) allyl ligand with a 1-*anti*,3-*syn*-comformation at atoms C3 and C5: C3–C4 = 1.401(3) Å, C4–C5 = 1.418(3) Å, at the bridging Ru atom Ru4,

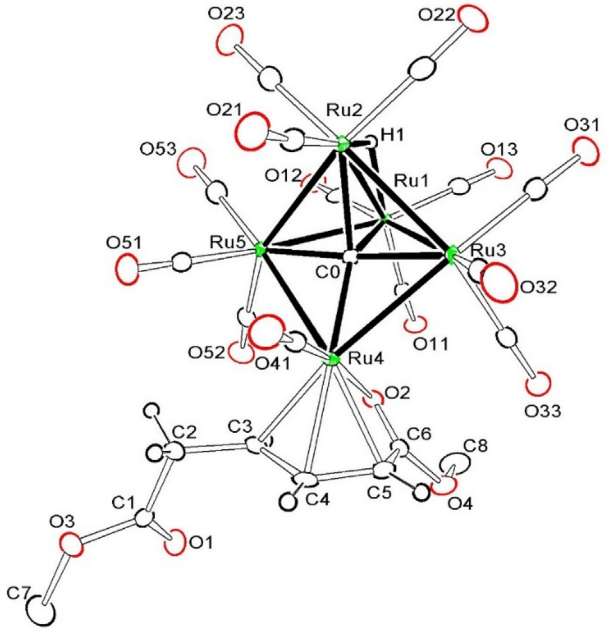

Fig. 2. ORTEP diagram of the molecular structure of $Ru_5(\mu_5\text{-}C)(CO)_{13}[\eta^3\text{-}1\text{-}anti, 3\text{-}syn\text{-}(MeO_2C)CH_2C_3H_3–CH_2\text{-}\eta^1\text{-}O{=}C(OMe)](\mu\text{-}H)$, **9**, showing 45% thermal ellipsoid probability. The hydrogen atoms on the methyl groups are omitted for clarity. Selected interatomic bond distances (Å) are as follows: Ru1–Ru3 = 2.8612(3), Ru1–Ru5 = 2.8553(3), Ru1–Ru2 = 2.8391(3), Ru2–Ru5 = 2.8328(3) Ru2–Ru3 = 2.8590(3), Ru3–Ru4 = 2.9222(2), Ru4–Ru5 = 2.8698(3), Ru1–H1 = 1.76(3), Ru2–H1 = 1.72(3), Ru4–O2 = 2.2904(15), Ru4–C3 = 2.228(2), Ru4–C4 = 2.180(2), Ru4–C5 = 2.192(2), C1–C2 = 1.516(3), C2–C3 = 1.503(3), C3–C4 = 1.401(3), C4–C5 = 1.418(3), C5–C6 = 1.464(3), C6–O2 = 1.231(3).

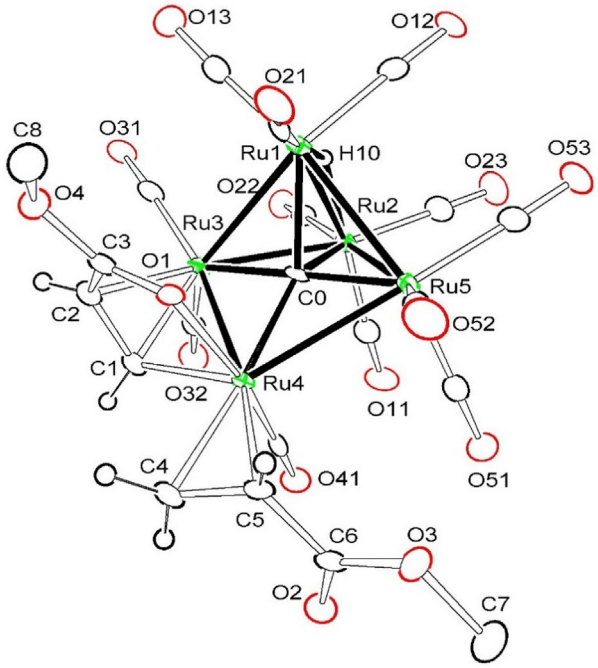

Fig. 3. ORTEP diagram of the molecular structure of $Ru_5(\mu_5\text{-}C)(CO)_{12}[\mu\text{-}\eta^3\text{-}O{=}C(OMe)CH{=}CH][\eta^2\text{-}CH{=}CHCO_2Me](\mu\text{-}H)$, **10**, showing 35% thermal ellipsoid probability. The hydrogen atoms on the methyl groups are omitted for clarity. Selected interatomic bond distances (Å) are as follows: Ru1–Ru3 = 2.9441(6), Ru1–Ru5 = 2.8369(6), Ru1–Ru2 = 2.8200(6), Ru2–Ru5 = 2.8884(6) Ru2–Ru3 = 2.8263(6), Ru3–Ru4 = 2.7341(6), Ru4–Ru5 = 3.0065(6), Ru1–H10 = 1.72(6), Ru2–H10 = 1.66(5), Ru4–O1 = 2.196(3), Ru4–C1 = 2.027(5), Ru4–C4 = 2.173(5), Ru4–C5 = 2.176(5), Ru3–C1 = 2.149(5), Ru3–C2 = 2.260(5), C1–C2 = 1.410(7), C2–C3 = 1.451(7), C3–O1 = 1.247(6), C4–C5 = 1.405(7), C5–C6 = 1.485(7), C6–O2 = 1.199(6), C6–O3 = 1.342(6).

Ru4–C3 = 2.228(2) Å, Ru4–C4 = 2.180(2), Å, Ru4–C5 = 2.192(2) Å. The H atoms bonded to carbon atoms C3 and C4 are trans to one another, $^3J_{H\text{-}H} = 11$ Hz, while the H atoms on C4 and C5 are cis oriented, $^3J_{H\text{-}H} = 7$ Hz, in the η^3-allyl portion of the ligand. The methylene group at C2 is not contained in a ring as found in **8**, instead the carbonyl oxygen atom O2 on C6 is coordinated to Ru4 to form a four-membered ring, Ru4–O2 = 2.2904(15) Å.

An ORTEP diagram of the molecular structure of **10** is shown in Fig. 3. Compound **10** contains an open Ru_5C cluster just like the other complexes and also contains two acrylate ligands, but most interestingly, in this molecule the acrylate ligands are not coupled. One of the methyl acrylate ligands is a bridging η^3-ligand similar to that found in **6** which includes coordination of the carbonyl oxygen atom O1, Ru4–O1 = 2.196(3), Ru4–C1 = 2.027(5) Å, Ru3–C1 = 2.149(5) Å, Ru3–C2 = 2.260(5) Å, C1–C2 = 1.410(7) Å. The other methyl acrylate ligand is a coordinated in the classical η^2-π-fashion by the olefinic carbon atoms C4 and C5 to the Ru atom, Ru4, Ru4–C4 = 2.173(5) Å, Ru4–C5 = 2.176(5) Å. Compound **10** also contains a bridging hydrido ligand across the hinge metal atoms Ru1 and Ru2, Ru1–H10 = 1.72(6) Å, Ru2–H10 = 1.66(5) Å, $\delta = -20.92$. With twelve terminal carbonyl ligands, a five-electron $\mu\text{-}\eta^3$-acryloyl ligand, a π-bonded methyl acrylate ligand, and a bridging hydrido ligand, the cluster contains a total valence electron count at the metal atoms of 76 cluster valence electrons, as expected for an open square pyramidal cluster of five metal atoms [17].

It seems like a simple addition of CO to **10** would lead to coupling of the acrylate ligands with the formation of one or more of the coupled products **8**, **9** and **11**. However, this was not

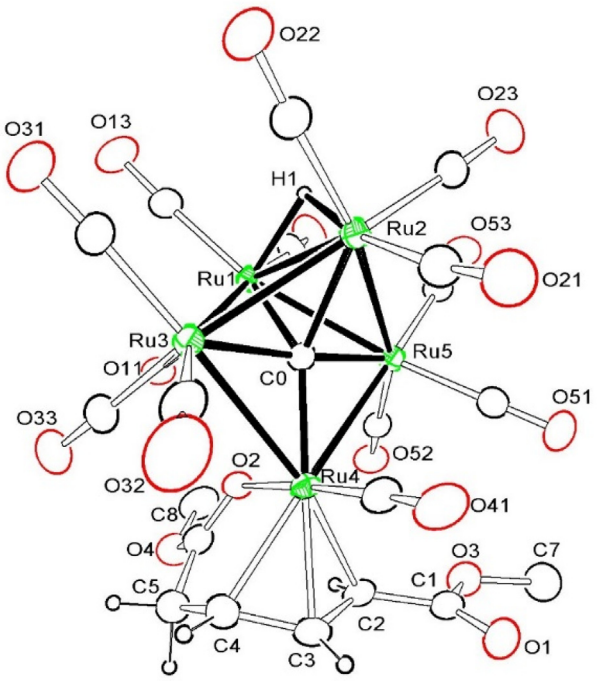

Fig. 4. ORTEP diagram of the molecular structure of $Ru_5(\mu_5\text{-}C)(CO)_{13}[\eta^3\text{-}1\text{-}syn, 3\text{-}anti\text{-}(MeO_2C)C_3H_3\text{-}\eta^1\text{-}O{=}C(OMe)CH_2](\mu\text{-}H)$, **11**, showing 20% thermal ellipsoid probability. The hydrogen atoms on the methyl groups are omitted for clarity. Selected interatomic bond distances (Å) are as follows: Ru1–Ru3 = 2.8401(5), Ru1–Ru5 = 2.8738(5), Ru1–Ru2 = 2.8322(5), Ru2–Ru5 = 2.8546(5) Ru2–Ru3 = 2.8691(5), Ru3–Ru4 = 2.9239(5), Ru4–Ru5 = 2.8950(6), Ru1–H1 = 1.84(5), Ru2–H1 = 1.76(4), Ru4–O2 = 2.197(3), Ru4–C2 = 2.235(5), Ru4–C3 = 2.191(5), Ru4–C4 = 2.255(5), C1–O1 = 1.203(6), C1–O3 = 1.348(7), C1–C2 = 1.463(7), C2–C3 = 1.422(8), C3–C4 = 1.393(7), C4–C5 = 1.521(9), C5–C6 = 1.481(9), C6–O2 = 1.233(6).

observed. All attempts to add CO to **10** resulted in replacement of the η^2-π-acrylate ligand by a CO ligand and formation of compound **7b**.

An ORTEP diagram of isomer **11** is shown in Fig. 4. The two methyl acrylate units in **11** are also tail-to-tail coupled to form a disubstituted η^3-allyl ligand $(MeO_2C)\text{-}\eta^3\text{-}C_3H_3\text{-}\eta^1\text{-}O{=}C(OMe)CH_2$ which has a 1-*syn*, 3-*anti* conformation of the substitutents, C2–C3 = 1.422(8) Å, C3–C4 = 1.393(7) Å, at the bridging Ru atom Ru4, Ru4–C2 = 2.235(5) Å, Ru4–C3 = 2.191(5) Å, 2.255(5) Å. The H atoms of C2 and C3 of **11** have a trans relationship, $^3J_{H\text{-}H} = 12$ Hz, while the H atom of C3 is cis to the H atom of C4, $^3J_{H\text{-}H} = 8$ Hz. The methylene group C5 is contained within a five-membered ring of atoms Ru4–O2–C6–C5–C4 formed by coordination of the oxygen atom O2 to Ru4, Ru4–O2 = 2.197(3) Å. Brookhart observed the formation of a similarly-coupled and π–allyl coordinated dimer of methyl acrylate in their studies of the reaction of methyl acrylate with $Cp^*Rh(C_2H_4)_2$ [5a].

To determine the relative stability of the three olefin coupled products **8**, **9** and **11**, solutions of pure samples of **8** and **9** in d_8-toluene solvent were heated to 80 °C. The isomerizations of the compounds were monitored by ^{1}H NMR spectroscopy for 25 h and 34 h respectively by observing the resonances of the hydrido ligands. Fig. 5 shows the changes in the ^{1}H NMR spectra of the isomerization of **8** as a function of time. As can be seen, compound **8** disappears completely within 25 h and is converted almost completely to **11**, but interestingly, small amounts of **9** are formed during this period before it too is converted to **11**.

The isomerization of **9** at 80 °C is shown in Fig. 6. As with **8**, it was observed that **9** was converted to **11**, but small amounts of **8** were formed in the process. These experiments demonstrate the compound **11** is the most stable of the three isomers. Interestingly, the studies show that **8** and **9** are interconverted en route to **11**

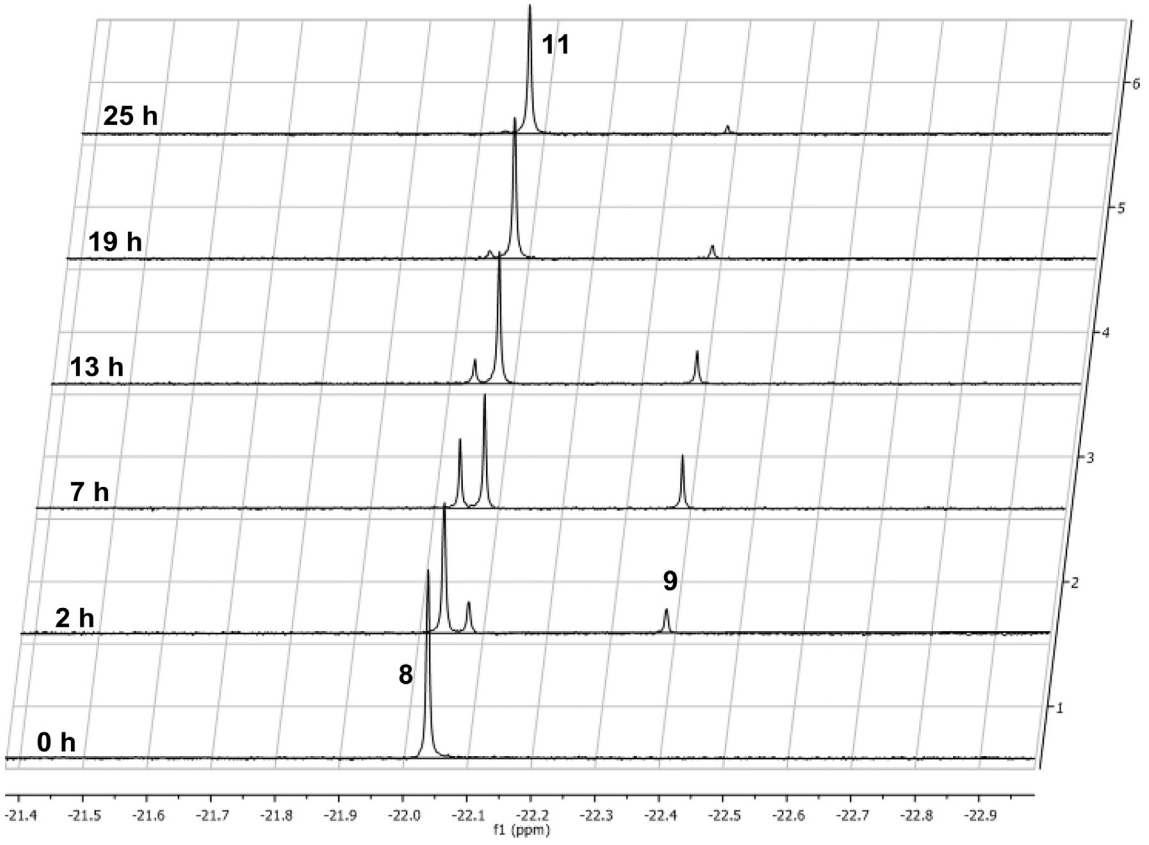

Fig. 5. Stacked plot of the ^{1}H NMR spectra in the hydride region in d_8-toluene showing the isomerization of compound **8** at 80 °C. Note the formation of transient amounts of **9**.

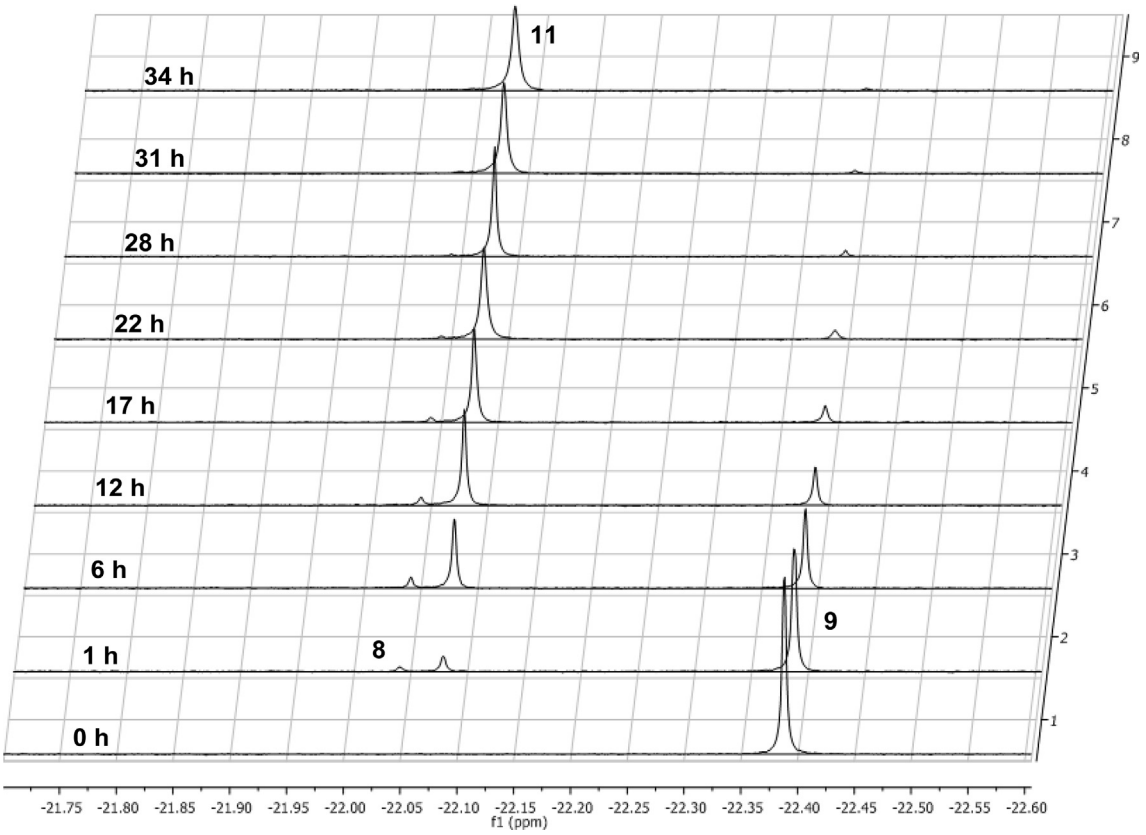

Fig. 6. Stacked plot of the ^{1}H NMR spectra in the hydride region in d_8-toluene showing the isomerization of compound **9** to **11** at 80 °C. Note the formation of transient amounts of **8**.

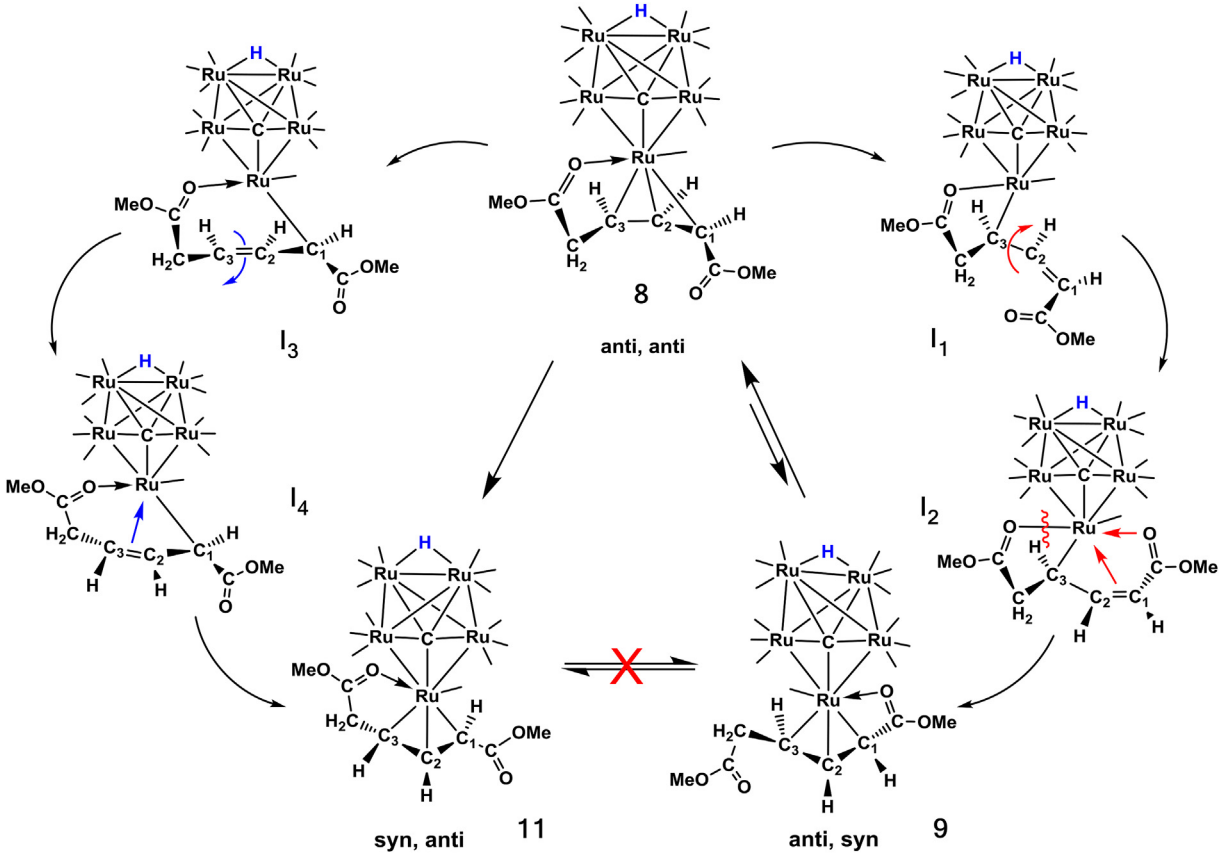

Scheme 5. Proposed mechanisms for the interconversion of the isomers **8**, **9** and **11.**

indicating that they must be fairly similar in energy.

The isomerization of η^3-allyl ligands is a well-known process through which the *syn* and *anti* substituents on an (η^3) σ-π allyl ligand are exchanged via conversion to an η^1-(σ)-allyl group followed by rotation around the newly formed carbon-carbon single bond and reformation of the new (η^3) σ-π allyl coordination mode [16]. Utilizing this established mechanism, rearrangements for the interconversion between compounds **8**, **9** and **11** can be explained as shown in Scheme 5. Assuming compound **8** is the first formed product in the original synthesis, it is converted into **9** by cleaving the Ru−C bonds to C1 and C2 of the allyl portion of the ligand to form the η^1-(σ)allyl intermediate $\mathbf{I_1}$. A 180° rotation about the C2 − C3 bond would generate the intermediate $\mathbf{I_2}$ which could then yield the isomer **9** by recoordination of the C1 − C2 double bond to the ruthenium atom, coordination of the carboxylate substituent on C1 and de-coordination of the carboxylate substituent on the CH_2 group. Note: It is not possible to transform **9** to **11** in one step by the π-σ-π *syn-anti* exchange mechanism. This isomerization of **9** to **11** must proceed by the reverse of the **8** to **9** transformation described above which then proceeds to **11** via the intermediates $\mathbf{I_3}$ and $\mathbf{I_4}$ as shown in Scheme 5 which also accounts for the observation of small amounts of **8** in the isomerization of **9** to **11**, Fig. 6. This mechanism is consistent with all of the spectral changes shown in Figs. 5 and 6.

The reaction of **6** with excess N,N-dimethylacrylamide at 98 °C for 11.5 h yielded two new tail-to-tail coupled dimethylacrylamide complexes: $Ru_5(\mu_5\text{-}C)(CO)_{13}[\eta^3\text{-}1\text{-}syn, 3\text{-}anti\text{-}Me_2NC{=}O{-}C_3H_3\text{-}\eta^1\text{-}O{=}CNMe_2CH_2](\mu\text{-}H)$, **12** in 18% yield and $Ru_5(\mu_5\text{-}C)(CO)_{13}[\eta^3\text{-}1\text{-}anti, 3\text{-}syn\text{-}(Me_2N)C(=O){-}C_3H_3{-}CH_2\text{-}\eta^1\text{-}O{=}C(NMe_2)](\mu\text{-}H)$, **13** in 22% yield. An ORTEP diagram of the molecular structure of **12** is shown in Fig. 7. The structure of **12** is analogous to that of the coupled methyl acrylate complex **10** except that **12** is formed from the coupling of two dimethylamido-substituted vinyl ligands.

Compound **12** contains a η^3-1-*syn*, 3-*anti*-$(Me_2NC{=}O)C_3H_3(\eta^1\text{-}O{=}CNMe_2CH_2)$ allylic ligand, C2−C3 = 1.406(6) Å, C3−C4 = 1.399(6) Å, formed by the coupling of two acrylamide molecules that is coordinated to the bridging metal atom Ru4, Ru4−C2 = 2.260(4) Å, Ru4−C3 = 2.177(4) Å, Ru4−C4 = 2.222(4) Å of an open Ru_5C cluster. A hydrido ligand spans the hinge metal atoms Ru1 and Ru2 of the Ru_4 portion of the cluster, Ru1−H1 = 1.77(4) Å, Ru2−H1 = Å, $\delta = -22.43$.

Compound **13**, an isomer of **12**, was also isolated and fully characterized structurally. An ORTEP diagram of the molecular structure of **13** is shown in Fig. 8. The molecular structure of **13** is analogous to that of **9** except the allylic ligand in **13** is formed by the coupling of two dimethylacrylamide ligands through the carbon atoms C3 and C4, C3−C4 = 1.392(7) Å, C2−C3 = 1.418(7) Å. The allylic ligand is coordinated to Ru4, Ru4−C2 = 2.200(5) Å, Ru4−C3 = 2.186(5) Å, Ru4−C4 = 2.218(5) Å and it has a η^3-1-*anti*, 3-*syn*-$Me_2NC{=}O{-}C_3H_3{-}CH_2\text{-}\eta^1\text{-}O{=}CNMe_2$ conformation. One of the amido groups is coordinated to Ru4 by the carbonyl group, Ru4−O1 = 2.215(3) Å.

The formation of a tail-to-tail olefin-coupled product by using different olefins was obtained from the reaction of **6** with methyl acrylate. A benzene solution containing **6** and an excess of methyl

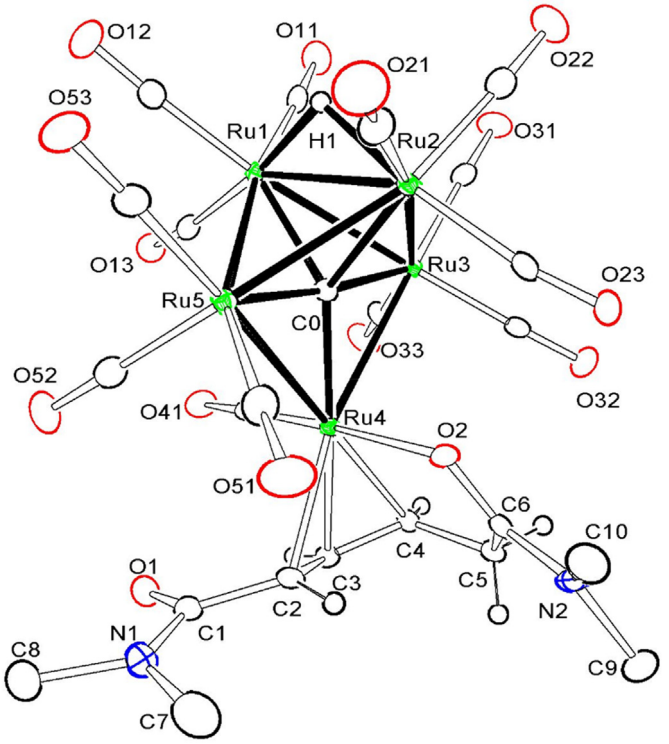

Fig. 7. ORTEP diagram of the molecular structure of $Ru_5(\mu_5\text{-}C)(CO)_{13}[\eta^3\text{-}1\text{-}syn, 3\text{-}anti\text{-}Me_2NC{=}O{-}C_3H_3\text{-}\eta^1\text{-}O{=}CNMe_2CH_2](\mu\text{-}H)$, **12**, showing 35% thermal ellipsoid probability. The hydrogen atoms on the methyl groups are omitted for clarity. Selected interatomic bond distances (Å) are as follows: Ru1−Ru3 = 2.8623(5), Ru1−Ru5 = 2.8540(5), Ru1−Ru2 = 2.8450(5), Ru2−Ru5 = 2.8534(5) Ru2−Ru3 = 2.8258(5), Ru3−Ru4 = 2.9339(5), Ru4−Ru5 = 2.9082(5), Ru1−H1 = 1.77(4), Ru2−H1 = 1.77(4), Ru4−O2 = 2.138(3), Ru4−C2 = 2.260(4), Ru4−C3 = 2.177(4), Ru4−C4 = 2.222(4), C1−C2 = 1.486(6) C2−C3 = 1.406(6), C3−C4 = 1.399(6), C4−C5 = 1.513(6), C5−C6 = 1.502(6), C6−N2 = 1.263(5).

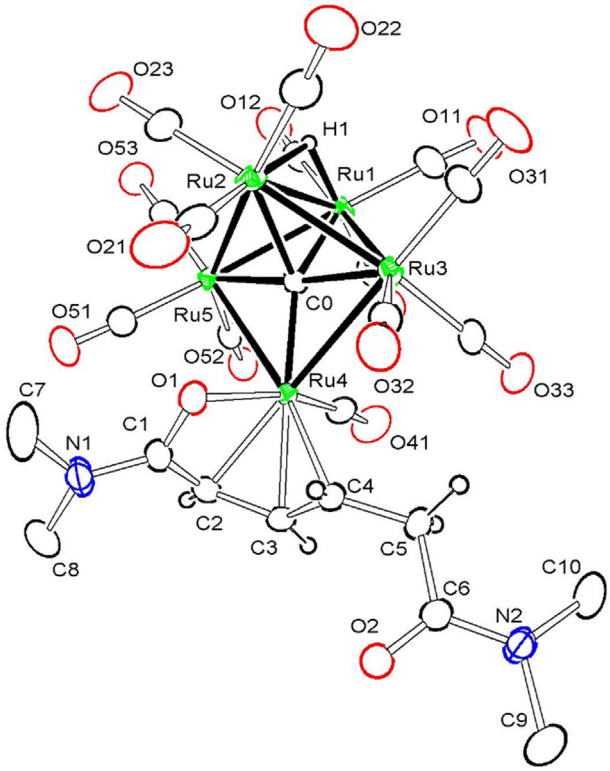

Fig. 8. ORTEP diagram of the molecular structure of $Ru_5(\mu_5\text{-}C)(CO)_{13}[\eta^3\text{-}1\text{-}anti, 3\text{-}syn\text{-}(Me_2N)C(=O){-}C_3H_3{-}CH_2\text{-}\eta^1\text{-}O{=}C(NMe_2)](\mu\text{-}H)$, **13**, showing 20% thermal ellipsoid probability. The hydrogen atoms on the methyl groups are omitted for clarity. Selected interatomic bond distances (Å) are as follows: Ru1−Ru3 = 2.8623(5), Ru1−Ru5 = 2.8224(5), Ru1−Ru2 = 2.8407(6), Ru2−Ru5 = 2.8599(5) Ru2−Ru3 = 2.8250(6), Ru3−Ru4 = 2.8912(5), Ru4−Ru5 = 2.9525(5), Ru1−H1 = 1.62(5), Ru2−H1 = 1.83(5), Ru4−O1 = 2.215(3), Ru4−C2 = 2.200(5), Ru4−C3 = 2.186(5), Ru4−C4 = 2.218(5), C1−O1 = 1.272(6), C1−C2 = 1.461(8), C2−C3 = 1.418(7), C3−C4 = 1.392(7), C4−C5 = 1.496(6), C5−C6 = 1.520(7).

acrylate was refluxed for 46 h at 80 °C to yield two new hetero-substituted olefin products: $Ru_5(\mu_5\text{-}C)(CO)_{12}[\mu\text{-}\eta^3\text{-}O{=}C(NMe_2)CH{=}CH][\eta^2\text{-}CH{=}CH(CO_2Me)](\mu\text{-}H)$, **14** in 3% yield, and $Ru_5(\mu_5\text{-}C)(CO)_{13}[\eta^3\text{-}1\text{-}anti,\ 3\text{-}syn\text{-}MeO_2CCH_2C_3H_3\text{-}\eta^1\text{-}O{=}C(NMe_2)](\mu\text{-}H)$, **15** in 30% yield. Compounds **14** and **15** were both fully characterized by a combination of IR, ^{1}H NMR, mass spectrometry and single-crystal X-ray diffraction. An ORTEP diagram of the molecular structure of **15** is shown in Fig. 9. Compound **14** is similar to **10** in that it contains two substituted olefins (one that is metallated) that are not coupled to each other. The dimethylacrylamido fragment is coordinated in a $\mu\text{-}\eta^2$-bridging fashion across metal atoms Ru4 and Ru5, Ru4–C1 = 2.016(6) Å, Ru5–C1 = 2.169(6) Å, Ru5–C2 = 2.275(6) Å. Ru4 is also coordinated to the amido carbonyl oxygen atom O1, Ru4–O1 = 2.153(4) Å. The second olefinic ligand is coordinated in the conventional η^2-olefinic manner, Ru4–C4 = 2.185(6) Å, Ru4–C5 = 2.190(6) Å, C4–C5 = 1.389(9) Å of the open Ru_5C cluster. Compound **14** also contains a bridging hydrido ligand across the hinge metal atoms Ru1 and Ru2 of the cluster, Ru1–H10 = 1.71(6) Å, Ru2–H10 = 1.79(6) Å, $\delta = -20.94$. With twelve terminal carbonyl ligands, a five-electron $\mu\text{-}\eta^3$-acryl-amido ligand, a π-bonded acrylate ligand, and a bridging hydride the total cluster valence electron count for **14** is 76 electrons [17].

An ORTEP diagram of the molecular structure of **15** is shown in Fig. 10. Compound **15** is similar in structure to compounds **9** and **13**. Compound **15** contains a η^3-1-*anti*, 3-*syn*-$MeO_2CCH_2C_3H_3\text{-}\eta^1$-O=C($NMe_2$) ligand, C2–C3 = 1.422(8) Å, C3–C4 = 1.393(7) Å, Ru4–C2 = 2.235(5) Å, Ru4–C3 = 2.191(5) Å, Ru4–C4 = 2.255(5) Å, formed by a tail-to-tail coupling of dimethylacrylamide and methyl acrylate in an open Ru_5C cluster. The carbonyl oxygen atom O1 of the dimethylformamido group is coordinated to Ru4, Ru4–O1 = 2.153(4) Å, while the MeO_2CCH_2 group on the η^3-allyl ligand is not coordinated.

To explore the nature of the effects of substitutents on olefinic C–H activations in activated olefins further, the reaction of compound **3** with vinyl acetate was also investigated. At this time, no examples of coupling between the C–H activated vinyl acetate ligand and another vinyl acetate by a metal complex have been reported. When compound **3** was treated with vinyl acetate at room temperature in the presence of Me_3NO (a CO removal reagent), the new compound $Ru_5(\mu_5\text{-}C)(CO)_{12}[\mu\text{-}\eta^2\text{-}(MeO_2C)CH{=}CH][\eta^3\text{-}CH_2{=}CHOC(=O)Me)](\mu\text{-}H)$, **16** was obtained in a very low yield (3%), see Scheme 6.

Compound **16** was characterized by a combination of IR, ^{1}H NMR, mass spectrometry and single-crystal X-ray diffraction. An ORTEP diagram of the molecular structure of **16** is shown in Fig. 11. Compound **16** contains two uncoupled vinyl acetate ligands that are coordinated similarly to uncoupled olefinic ligands in compounds **10** and **14**, see above. One of ligands is a $\mu\text{-}\eta^2$-$(MeCO_2)CH{=}CH$ bridging vinyl ligand that is metallated at C3, the β-carbon atom, Ru4–C3 = 2.0633(19) Å. Its olefinic group is coordinated in a π-fashion to the metal atom Ru3, Ru3–C3 = 2.1792(19) Å, Ru3–C4 = 2.2724(19), Å, C3–C4 = 1.391(3) Å and a σ–fashion to Ru4, Ru4–C3 = 2.0633(19) Å. The H atoms on C3 and C4 are trans-oriented; $^3J_{H\text{-}H} = 9.0$ Hz in the ^{1}H NMR spectrum. Evidently, there was a shift of one of the hydrogen atoms from the exo-CH_2 group in the parent **3** to the α-carbon C4 in the transformation to **16**. The

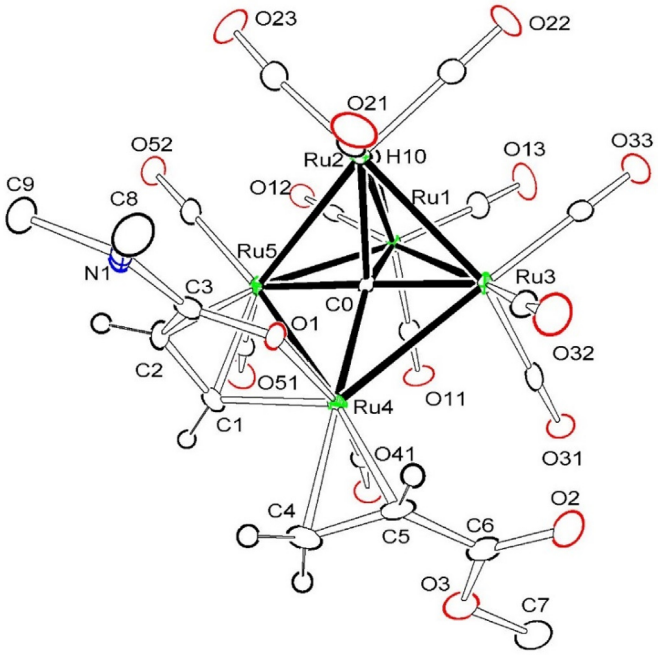

Fig. 9. ORTEP diagram of the molecular structure of $Ru_5(\mu_5\text{-}C)(CO)_{12}[\mu\text{-}\eta^3\text{-}O{=}C(NMe_2)CH{=}CH][\eta^2\text{-}CH{=}CHCO_2Me](\mu\text{-}H)$, **14** showing 35% thermal ellipsoid probability. Selected interatomic bond distances (Å) are as follows: Ru1–Ru3 = 2.8643(6), Ru1–Ru5 = 2.8317(6), Ru1–Ru2 = 2.8151(6), Ru2–Ru5 = 2.9536(6) Ru2–Ru3 = 2.8287(6), Ru3–Ru4 = 3.0149(6), Ru4–Ru5 = 2.7359(6), Ru1–H10 = 1.71(6), Ru2–H10 = 1.79(6), Ru4–O1 = 2.153(4), Ru4–C1 = 2.016(6), Ru4–C4 = 2.185(6), Ru4–C5 = 2.190(6), Ru5–C1 = 2.169(6), Ru5–C2 = 2.275(6), C1–C2 = 1.415(9) C2–C3 = 1.467(8), C3–O1 = 1.278(7), C4–C5 = 1.389(9), C5–C6 = 1.482(9), C6–O2 = 1.210(8), C6–O3 = 1.339(7), Ru1–C0 = 2.116(5), Ru2–C0 = 2.096(5), Ru3–C0 = 1.942(5), Ru4–C0 = 2.107(5), Ru5–C0 = 1.968(5).

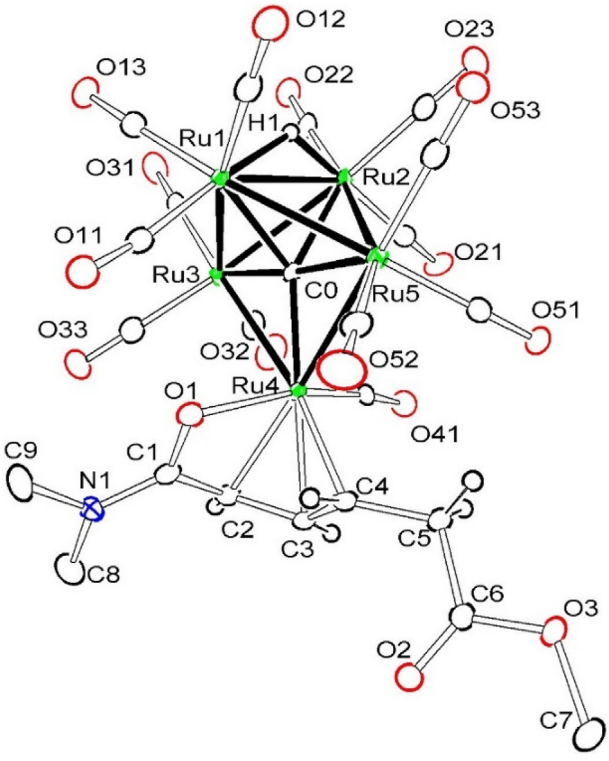

Fig. 10. ORTEP diagram of the molecular structure of $Ru_5(\mu_5\text{-}C)(CO)_{13}[\eta^3\text{-}1\text{-}anti,\ 3\text{-}syn\text{-}MeO_2CCH_2C_3H_3\text{-}\eta^1\text{-}O{=}C(NMe_2)](\mu\text{-}H)$, **15**, showing 20% thermal ellipsoid probability. The hydrogen atoms on the methyl groups are omitted for clarity. Selected interatomic bond distances (Å) are as follows: Ru1–Ru3 = 2.8401(5), Ru1–Ru5 = 2.8738(5), Ru1–Ru2 = 2.8322(5), Ru2–Ru5 = 2.8546(5) Ru2–Ru3 = 2.8691(5), Ru3–Ru4 = 2.9239(5), Ru4–Ru5 = 2.8950(6), Ru1–H1 = 1.84(4), Ru2–H1 = 1.76(4), Ru4–O2 = 2.197(3), Ru4–C2 = 2.235(5), Ru4–C3 = 2.191(5), Ru4–C4 = 2.255(5), C1–C2 = 1.463(7), C2–C3 = 1.422(8), C3–C4 = 1.393(7), C4–C5 = 1.521(9), C5–C6 = 1.481(9), C6–O2 = 1.233(6), Ru1–C0 = 2.139(4), Ru2–C0 = 2.138(4), Ru3–C0 = 1.980(4), Ru4–C0 = 2.043(4), Ru5–C0 = 1.973(4).

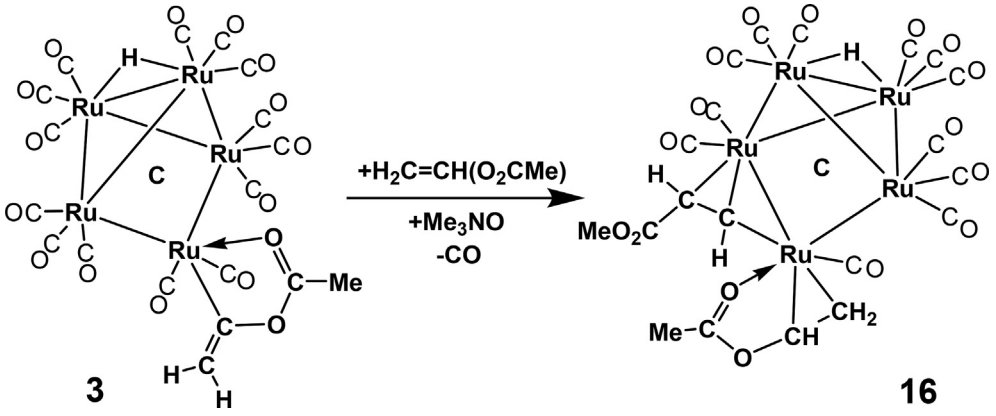

Scheme 6. A schematic of the formation of compound **16** from the reaction of **3** with vinyl acetate.

mechanism for this rearrangement is not known at this time. The added vinyl acetate ligand has not undergone a CH bond activation and it exhibits the conventional face-bonded π-olefin coordination to the ruthenium atom Ru4, Ru4—C1 = 2.176(2) Å, Ru4—C2 = 2.1208(19) Å, C1—C2 = 1.394(3) Å. However, unlike compounds **10** and **14**, the substituent of this π-vinyl acetate ligand is coordinated to a metal atom, Ru4, by the oxygen atom O1 of the acetate carbonyl group, Ru4—O1 = 2.1725(14) Å. A similarly coordinated chelating π-vinyl acetate ligand was observed in the complex $Os_3(CO)_{10}[\eta^3\text{-}H_2C{=}CH(O_2CMe)]$ [18]. With twelve terminal carbonyl ligands, a three-electron donating μ-η^2-vinyl acetate ligand, a four-electron η^3-π-vinyl acetate substituted ligand, and a bridging hydride, complex **16** contains a total valence electron count of 76 electrons. This is consistent with the observed, open structure for this Ru_5 cluster [17].

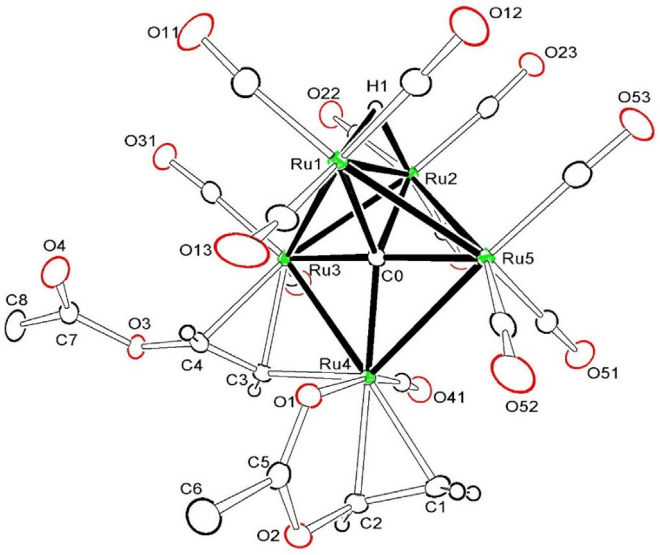

Fig. 11. ORTEP diagram of the molecular structure of $Ru_5(\mu_5\text{-}C)(CO)_{12}[\mu\text{-}\eta^2\text{-}(MeO_2C)CH{=}CH][\eta^3\text{-}CH_2{=}CHOC(=O)Me)](\mu\text{-}H)$, **16** showing 50% thermal ellipsoid probability. Selected interatomic bond distances (Å) are as follows: Ru1—Ru3 = 2.9414(2), Ru1—Ru5 = 2.8577(2), Ru1—Ru2 = 2.8433(2), Ru2—Ru5 = 2.8524(2) Ru2—Ru3 = 2.8576(2), Ru3—Ru4 = 2.7674(2), Ru4—Ru5 = 2.9575(2), Ru1—H1 = 1.82(2), Ru2—H1 = 1.74(2), Ru4—O1 = 2.1725(14), Ru4—C1 = 2.176(2), Ru4—C2 = 2.1208(19), Ru4—C3 = 2.0633(19), Ru3—C3 = 2.1792(19), Ru3—C4 = 2.2724(19), C1—C2 = 1.394(3), C3—C4 = 1.391(3).

4. Summary and conclusions

In this work, it has been shown that polar vinyl olefins can be added to the pentaruthenium carbonyl complexes **1**, **2**, **3** and **6**. In general, the added olefinic ligand undergoes tail-to-tail C—C bond-forming coupling and cross-coupling reactions that proceed to the formation of disubstituted η^3-allyl ligands that are coordinated to the bridging ruthenium atom of an open Ru_5 carbonyl cluster complex. These allyl ligands isomerize via the conventional π-σ-π mechanisms to yield other stable isomers. Three diolefin complexes **10**, **14**, and **16** were obtained in which the olefins were not coupled. While it seems that these diolefin complexes should be precursors to the olefin-coupled complexes, we have not yet been able to obtain any of the C—C coupled products from them by simple treatments.

Accession codes

Files CCDC 1946438—1946446 with the Cambridge Crystallographic Data Centre contain the supplementary crystallographic data for the compounds **8**—**16** in this report. These data can be obtained free of charge via www.ccdc.cam.ac.uk/data_request/cif, or by emailing data_request@ccdc.cam.ac.uk, or by contacting The Cambridge Crystallographic Data Centre, 12 Union Road, Cambridge CB2 1EZ, UK; fax: +44 1223 336033.

Notes

The authors declare no competing financial interest.

Acknowledgments

This research was supported by grant 1764192 from the National Science Foundation.

Appendix A. Supplementary data

Supplementary data to this article can be found online at https://doi.org/10.1016/j.jorganchem.2019.120938.

References

[1] (a) J.A. Brydson, in: Plastics Materials, seventh ed., Butterworth Heinemann Pubs., Oxford, 2000. Ch. 15;
(b) E. Penzel, E, in: B. Elvers (Ed.), Ullmann's Polymers and Plastics: Products and Processes, vol 2, Wiley-VCH Verlag GmbH & Co KGaA, Weinheim, 2016, pp. 675—696, https://doi.org/10.1002/14356007.a21_157. Polyacrylates;
(c) A. Zarrouki, E. Espinosa, C. Boisson, V. Monteil, Free radical

copolymerization of ethylene with vinyl acetate under mild conditions, Macromolecules 50 (2017) 3516–3523;
(d) K.W. Doak, in: second ed., in: H.F. Mark, N.M. Bikales, C.G. Overberger, G. Menges (Eds.), Encyclopedia of Polymer Science and Engineering, vol 6, Wiley, New York, 1986, pp. 386–429;
(e) H. Rinno, in: sixth ed., in: H. Ullmann's (Ed.), Encyclopedia of Industrial Chemistry, vol 29, Wiley-VCH, Weinheim, 2003, pp. 49–59.

[2] (a) E.Y.-X. Chen, Coordination polymerization of polar vinyl monomers by single-site metal catalysts, Chem. Rev. 109 (2009) 5157–5214;
(b) D. Guironnet, L. Caporaso, B. Neuwald, I. Göttker-Schnetmann, L. Cavallo, S. Mecking, Mechanistic insights on acrylate insertion polymerization, J. Am. Chem. Soc. 132 (2010) 4418–4426;
(c) H. Yasuda, Organo-rare-earth-metal initiated living polymerizations of polar and nonpolar monomers, J. Organomet. Chem. 647 (2002) 128–138;
(d) E. Ihara, M. Morimoto, H. Yasuda, Living polymerizations and copolymerizations of alkyl acrylates by the unique catalysis of rare earth metal complexes, Macromolecules 28 (1995) 7886–7892;
(e) M. Tanabe, T. Sugimura, H. Yasuda, Maximization of the molecular weight of poly[alkyl(meth)acrylate] using $SmMe(C_5Me_5)_2(THF)$ as an Initiator, React. Funct. Polym. 52 (2002) 135–141.

[3] (a) Z. Chen, M. Brookhart, M, Exploring ethylene/polar vinyl monomer copolymerizations using Ni and Pd α-diimine catalysts, Acc. Chem. Res. 51 (2018) 1831–1839;
(b) Y. Zhang, H. Mu, L. Pan, X. Wang, Y. Li, Robust bulky [P,O] neutral nickel catalysts for copolymerization of ethylene with polar vinyl monomers, ACS Catal. 8 (2018) 5963–5976;
(c) A. Nakamura, A, T.M.J. Anselment, J. Claverie, B. Goodall, R.F. Jordan, S. Mecking, B. Rieger, A. Sen, A, P.W.N.M. van Leeuwen, K. Nozaki, Ortho-phosphinobenzenesulfonate: a superb ligand for palladium-catalyzed Coordination–Insertion copolymerization of polar vinyl monomers, Acc. Chem. Res. 46 (2013) 1438–1449;
(d) X. Sui, S. Dai, C. Chen, Ethylene polymerization and copolymerization with polar monomers by cationic phosphine phosphonic amide palladium complexes, ACS Catal. 5 (2015) 5932–5937;
(e) D. Guironnet, P. Roesle, T. Rünzi, I. Göttker-Schnetmann, S. Mecking, Insertion polymerization of acrylate, J. Am. Chem. Soc. 131 (2009) 422–423;
(f) S. Mecking, L.K. Johnson, L. Wang, M. Brookhart, Mechanistic studies of the palladium-catalyzed copolymerization of ethylene and α-olefins with methyl acrylate, J. Am. Chem. Soc. 120 (1998) 888–899;
(g) E. Drent, R. van Dijk, R. van Ginkel, B. van Oort, R.I. Pugh, Palladium catalysed copolymerisation of ethene with alkylacrylates: polar comonomer built into the linear polymer chain, Chem. Commun. (2002) 744–745;
(h) K.M. Skupov, P.R. Marella, M. Simard, G.P.A. Yap, N. Allen, D. Conner, B.L. Goodall, J.P. Claverie, Palladium aryl sulfonate phosphine catalysts for the copolymerization of acrylates with ethene, Macromol. Rapid Commun. 28 (2007) 2033–2038;
(i) T. Runzi, D. Guironnet, I. Gottker-Schnetmann, S. Mecking, Reactivity of methacrylates in insertion polymerization, J. Am. Chem. Soc. 132 (2010) 16623–16630;
(j) N. Schuster, T. Rünzi, S. Mecking, Reactivity of functionalized vinyl monomers in insertion copolymerization, Macromolecules 49 (2016) 1172–1179;
(k) B.L. Goodall, Late transition metal catalysts for the copolymerization of olefins and polar monomers, Top. Organomet. Chem. 26 (2009) 159–178;
(l) J. Gao, B. Yang, C. Chen, C. Sterics versus electronics: imine/phosphine-oxide-based nickel catalysts for ethylene polymerization and copolymerization, J. Catal. 369 (2019) 233–238.

[4] (a) A. Keyes, H.E. Basbug Alhan, E. Ordonez, U. Ha, D.B. Beezer, H. Dau, Y.-S. Liu, E. Tsogtgerel, G.R. Jones, E. Harth, Olefins and vinyl polar monomers: bridging the gap for next generation materials, Angew. Chem. Int. Ed. 58 (2019) 12370–12391;
(b) L.S. Boffa, B.M. Novak, Copolymerization of polar monomers with olefins using transition-metal complexes, Chem. Rev. 100 (2000) 1479–1494;
(c) A. Nakamura, S. Ito, K. Nozaki, Coordination–Insertion copolymerization of fundamental polar monomers, Chem. Rev. 109 (2009) 5215–5244;
(d) S. Ito, K. Munakata, A. Nakamura, K. Nozaki, Copolymerization of vinyl acetate with ethylene by palladium/alkylphosphine-sulfonate catalysts, J. Am. Chem. Soc. 131 (2009) 14606–14607;
(e) M. Chen, C. Chen, A versatile ligand platform for palladium- and nickel-catalyzed ethylene copolymerization with polar monomers, Angew. Chem. Int. Ed. 57 (2018) 3094–3098;
(f) R. Joshi, G. Zhang, J.T. Miller, R. Gounder, Evidence for the Coordination–Insertion mechanism of ethene dimerization at nickel cations exchanged onto beta molecular sieves, ACS Catal. 8 (2018) 11407–11422;
(g) P. Braunstein, C. Frison, X. Morise, Stepwise ethene and/or methyl acrylate/CO insertions into the Pd-C bond of cationic palladium(II) complexes stabilized by a (P,O) chelate, Angew. Chem. Int. Ed. 39 (2000) 2867–2870.

[5] (a) E. Hauptman, S. Sabo-Etienne, P.S. White, M. Brookhart, J.M. Gamer, P.J. Fagan, J.C. Calabrese, Design and study of Rh(III) catalysts for the selective tail-to-tail dimerization of methyl acrylate, J. Am. Chem. Soc. 116 (1994) 8038–8060;
(b) M. Brookhart, S. Sabo-Etienne, Catalytic tail-to-tail dimerization of methyl acrylate using rhodium (III) catalysts, J. Am. Chem. Soc. 113 (1991) 2777–2799;
(c) R.J. McKinney, Ruthenium-catalyzed acrylate dimerization, Organometallics 5 (1986) 1753–1755;
(d) R.J. McKinney, M.C. Colton, Homogeneous ruthenium-catalyzed acrylate dimerization. Isolation, characterization, and crystal structure of the catalytic precursor Bis(dimethyl muconate)-(trimethyl phosphite)ruthenium(0), Organometallics 5 (1986) 1080–1085;
(e) P. Braunstein, M.J. Chetcuti, R. Welter, Bimetallic-induced tail-to-tail dimerization and C–H activation of methyl acrylate, Chem. Commun. (2001) 2508–2509;
(f) S. Matsuoka, Y. Fukumoto, M. Suzuki, Tail-to-tail cross-dimerization of methyl methacrylate/methacrylonitrile with acrylates catalyzed by N-heterocyclic carbene, Chem. Lett. 46 (2017) 983–986;
(g) P. Pertici, V. Ballantini, P. Salvadori, M.A. Bennett, The Ru(η^6-naphthalene)(η^4-cycloocta-l,5-diene)/Acetonitrile system in the selective dimerization of methyl acrylate to frans-Dimethyl-2-hexenedioate, Organometallics 14 (1995) 2565–2569;
(h) M. Hirano, Y. Sakate, N. Komine, S. Komiya, M.A. Bennett, Isolation of trans-2,5 bis(methoxycarbonyl)ruthenacyclopentane by oxidative coupling of methyl acrylate on ruthenium(0) as an active intermediate for tail-to-tail selective catalytic dimerization, Organometallics 28 (2009) 4902–4905;
(i) J. Zimmermann, I. Tkatchenko, P. Wasserscheid, Mono- and bidentate phosphine ligands in the palladium-catalyzed methyl acrylate dimerization, Adv. Synth. Catal. 345 (2003) 402–409;
(j) G.M. DiRenzo, P.S. White, M. Brookhart, Mechanistic studies of catalytic olefin dimerization reactions using electrophilic η^3-allyl-palladium(II) complexes, J. Am. Chem. Soc. 118 (1996) 6225–6234;
(k) Y. Kaneko, T. Kanke, S. Kiyooka, K. Isobe, Selective tail-to-tail dimerization of ethyl acrylate catalyzed by dirhodium complexes, Chem. Lett. (1997) 23–24;
(l) G.L. Tembe, P.A. Ganeshpure, S. Satish, Catalytic tail-to-tail dimerization of methyl acrylate using bis(triphenylphosphine)tricarbonyl ruthenium(0), React. Kinet. Catal. Lett. 63 (1998) 151–156;
(m) X.-H. Hu, J. Zhang, X.F. Yang, Y.H. Xu, T.P. Loh, Stereo- and chemoselective cross-coupling between two electron-deficient acrylates: an efficient route to (Z,E)-Muconate derivatives, J. Am. Chem. Soc. 137 (2015) 3169–3172.

[6] (a) J. Zhang, T.-P. Loh, Ruthenium- and rhodium-catalyzed cross-coupling reaction of acrylamides with alkenes: efficient access to (Z,E)-dienamides, Chem. Commun. 48 (2012) 11232–11234;
(b) Y.-H. Xu, J. Lu, T.-P. Loh, Direct cross-coupling reaction of simple alkenes with acrylates catalyzed by palladium catalyst, J. Am. Chem. Soc. 131 (2009) 1372–1373;
(c) Y.-H. Xu, W.-J. Wang, Z.-K. Wen, J.-J. Hartley, Y.-H. Xu, Y.-K. Cho k, T.-P. Loh, Synthesis and characterization of a cyclic vinylpalladium(II) complex: vinylpalladium species as the possible intermediate in the catalytic direct olefination reaction of enamide, Chem. Sci. 2 (2011) 1822–1825;
(d) H. Yu, W. Jin, C. Sun, J. Chen, W. Du, S. He, Z. Yu, Palladium-catalyzed cross-coupling of internal alkenes with terminal alkenes to functionalized 1,3-butadienes using C-H bond activation: efficient synthesis of bicyclic pyridones, Angew. Chem. Int. Ed. 40 (2010) 5792–5797;
(e) T. Besset, N. Kuhl, F.W. Patureau, F. Glorius, Rh-III-Catalyzed oxidative olefination of vinylic C-H bonds: efficient and selective access to diunsaturated alpha-amino acid derivatives and other linear 1,3-butadienes, Chem. Eur J. 17 (2011) 7167–7171;
(f) Y. Zhang, Z. Cui, Z. Li, Z.-Q. Liu, Pd(II)-Catalyzed dehydrogenative olefination of vinylic C-H bonds with allylic esters: general and selective access to linear 1,3-butadienes, org, Letters 14 (2012) 1838–1841.

[7] Y. Hatamoto, S. Sakaguchi, Y. Ishii, Oxidative cross-coupling of acrylates with vinyl carboxylates catalyzed by a $Pd(OAc)_2$/HPMoV/O_2 system, Org. Lett. 6 (2004) 4623–4625.

[8] (a) B.S. Williams, M.D. Leatherman, P.S. White, M. Brookhart, Reactions of vinyl acetate and vinyl trifluoroacetate with cationic diimine Pd(II) and Ni(II) alkyl complexes: identification of problems connected with copolymerizations of these monomers with ethylene, J. Am. Chem. Soc. 127 (2005) 5132–5146;
(b) S. Komiya, T. Ito, M. Cowie, A. Yamamoto, J.A. Ibers, Carbon-hydrogen bond activation by transition metal complexes. Oxidative addition of alkyl methacrylate to ruthenium. The structure of hydrido(2-n-butoxycarbonylpropenyl-C1,0)tris-(triphenylphosphine) ruthenium(II), J. Am. Chem. Soc. 98 (1976) 3874–3884.

[9] R.D. Adams, M.D. Smith, J.D. Tedder, Substituent-directed activation of CH bonds in activated olefins by $Ru_5(\mu_5\text{-}C)(CO)_{15}$, Eur. J. Inorg. Chem. (2018) 2984–2986.

[10] R.D. Adams, M.D. Smith, J.D. Tedder, N.D. Wakdikar, Selective activation of CH bonds in polar vinyl olefins and coupling of ethylene to the activated carbon atoms in pentaruthenium complexes, Inorg. Chem. 58 (2019) 8357–8368.

[11] B.F.G. Johnson, J. Lewis, J.N. Nicholls, J. Puga, P.R. Raithby, M.J. Rosales, M. McPartlin, W. Clegg, The synthesis of $[Ru_5C(CO)_{15}]$ by the carbonylation of $]Ru_6C(CO)_{17}]$ and the reactions of the pentanuclear cluster with a variety of small molecules: the X-ray structure analyses of $[Ru_5C(CO)_{15})]$, $Ru_5C(CO_{15})$(-MeCN)], $[Ru_5C(CO)_{14}(PPh_3)]$, $[Ru_5C(CO_{13})(PPh_3)_2]$ and $[Ru_5(\mu\text{-}H)_2C(CO_{12})(Ph_2P(CH_2)_2PPh_2)]$, J. Chem. Soc. Dalton Trans. (1983) 277–290.

[12] R.D. Adams, J.D. Tedder, formation of N,N-dimethylacrylamide by a multicenter hydrocarbamoylation of C_2H_2 with N,N-dimethylformamide activated by $Ru_5(\mu_5\text{-}C)(CO)_{15}$, Inorg. Chem. 57 (2018) 5707–5710.

[13] SAINT+, Version 6.2a, Bruker Analytical X-ray Systems, Inc., Madison, WI, 2001.

[14] APEX3 Version 2016.5-0 and SAINT Version 8.34A. Bruker AXS, Inc. Madison, WI, USA.
[15] G.M. Sheldrick, SHELXTL, Version 6.1, Bruker Analytical X-ray Systems, Inc., Madison, WI, 1997.
[16] K. Vrieze, in: L.M. Jackman, F.A. Cotton (Eds.), Dynamic Nuclear Magnetic Resonance Spectroscopy, Academic Press, New York, 1975. Ch. 11, Sec. II.D.2.
[17] D.M.P. Mingos, A.S. May, in: D.F. Shriver, H.D. Kaesz, R.D. Adams (Eds.), The Chemistry of Metal Cluster Complexes, VCH Publishers, New York, 1990. Ch. 2.
[18] E. Boyar, A.J. Deeming, I.P. Rothwell, K. Henrick, M. McPartlin, Chelation of vinyl acetate and related unsaturated ketones: molecular structure of $[Os_3(CO)_{10}(CH_2{=}CHOCOMe)]$, J. Chem. Soc. Dalton Trans. (1986) 1437–1441.